

A new approach for parameters estimation of double and triple diode models of photovoltaic cells based on iterative Lambert W function



Martin Čalasan^a, Shady H.E. Abdel Aleem^{b,c,*}, Ahmed F. Zobaa^d

^a Faculty of Electrical Engineering, University of Montenegro, Montenegro

^b ETA Electric, Power Quality Solutions Department, 12111 Giza, Egypt

^c College of Engineering and Technology, Arab Academy for Science, Technology and Maritime Transport, Smart Village Campus, Giza 12577, Egypt

^d College of Engineering, Design & Physical Sciences, Brunel University London, Uxbridge, United Kingdom

ARTICLE INFO

Keywords:

Iterative Lambert W Optimization Parameter estimation Photovoltaic solar cells 7-parameter double diode model 9-parameter triple diode model

ABSTRACT

An approximated expression for the calculated solar cell current is usually used in parameters estimation of the 7-parameter double diode model (DDM) and the 9-parameter triple diode model (TDM) of solar photovoltaic (PV) equivalent circuits. Then the root mean square error (RMSE) is calculated between the measured and estimated values of the output current. In the mathematical sense, the RMSE calculation procedure is not correct. In this work, a novel iterative approach based on the Lambert W function is proposed to calculate the solar cell current in both DDM and TDM. Then, the RMSE values computed using the parameters found by many optimization algorithms presented in the literature are presented and discussed for the RTC France PV cell and Solarex MSX-60 PV module. The results obtained show that RMSE values were not accurately calculated in most of these methods. Further, an improved LSHADE optimization algorithm called Chaotic LSHADE algorithm is proposed to solve the 7-parameter and 9-parameter estimation problem of the PV equivalent circuits. The proposed methodology is also applied to current-voltage characteristics measured in the laboratory for solar modules of Clean Energy Trainer Setup. The 7 and 9 unknown parameters are estimated using the CLSHADE algorithm based on the minimization of the RMSE values calculated. The results

Abbreviations: ABC, artificial bee colony; ABC-KP, ABC key points; ABC-TRR, ABC-trust-region reflective; ABSO, artificial bee swarm optimization; BBO, biogeography-based optimization; BBO-M, BBO algorithm with mutation strategies; BFA, bacterial foraging algorithm; BPFP, bee pollinator FPA; BMO, bird mating optimization; BLPSO, biogeography-based learning PSO; BSA, backtracking search algorithm; CETS, Clean Energy Trainer Setup; CLPSO, comprehensive learning particle swarm optimization; CLSHADE, chaotic LSHADE; CMM-DE/BBO, DE/BBO with covariance matrix-based migration; COA, chaotic optimization approach; COOA, coyote optimization algorithm; CPSO, chaos PSO; CS, cuckoo search; CSO, competitive swarm optimization; CWOA, chaotic whale optimization algorithm; DDM, double diode model; DE, differential evolution; DE/BBO, hybrid DE with BBO; DET, DE technique; DGM, Dynamic Gaussian mutation; EAs, evolutionary algorithms; EDDM-LW, explicit double-diode model-Lambert W; EHA-NMS, eagle-based hybrid adaptive Nelder-Mead simplex algorithm; ELPSO, enhanced leader particle swarm optimisation; FA, firefly algorithm; FPA, flower pollination algorithm; GA, genetic algorithm; GABC, gbestguided ABC; GBABC, Gaussian bare-bones ABC; GGHS, grouping-based global HS; GOFPANM, generalized opposition-FPA-NM simplex method; GOTLBO, generalized oppositional teaching learning-based optimization; GWO, grey wolf optimization; HCLPSO, heterogeneous comprehensive learning PSO; HFAPS, hybrid FA and PS; HPSOSA, hybrid PSO and SA; HS, harmony search; IABC, improved ABC; IPEX, open-source C++ library for constraint processing over real numbers; IBEXOPT-MAE, IPEX optimization-based on MAE; IBEXOPT-SSE, IPEX optimization - based on SSE; ICA, imperialist competitive algorithm; IGHS, innovative global HS; IJAYA, improved JAYA; ImCSA, improved CS algorithm; ISCA, improved sine cosine algorithm; JAYA, word means victory (Sanskrit word); LB, lower bound; LBSA, learning BSA; LETLBO, TLBO with learning experience of other learners; LPSR, linear population size reduction; MABC, modified ABC; MAE, maximal absolute error; MJAYA, modified JAYA; MPCOA, mutative-scale parallel chaos optimization algorithm; MPSO, PSO with adaptive mutation strategy; MSSO, modified simplified swarm optimization algorithm; NIWTLBO, nonlinear inertia weighted TLBO; NM-MPSO, Nelder-Mead and modified PSO; OBWOA, opposition-based WOA; ODE, opposition-based DE; PGJAYA, performance-guided JAYA; PS, pattern search; pSFS, perturbed stochastic fractal search; PSO, particle swarm optimization; PV, photovoltaic; R-II, Rao-2; R-III, Rao-3; Rcr-IJADE, rate crossover repairing improved adaptive DE; RTLBO, ranking TLBO; SA, simulated annealing; SATLBO, self-adaptive TLBO; SDM, single diode model; SFO, sunflower optimization; SFS, stochastic fractal search; SHADE, success-history based adaptive DE; SSE, sum of squared error; SSO, simplified swarm optimization; STLBO, simplified TLBO; TDM, triple diode model; TLABC, teaching-learning-based ABC; TLBO, teaching-learning-based optimization; TLO, teaching-learning optimization; TVACPSO, time-varying acceleration coefficients PSO; UB, upper bound; WCA, water cycle algorithm; WLCSODGM, winner-leading CSO with DGM; WOA, whale optimization algorithm.

* Corresponding author at: ETA Electric, Power Quality Solutions Department, 12111 Giza, Egypt.

E-mail addresses: martinc@ucg.ac.me (M. Čalasan), engyshady@ieee.org (S.H.E. Abdel Aleem), azobaa@ieee.org (A.F. Zobaa).

obtained show that the proposed algorithm achieves better solutions than the solutions obtained by many optimization algorithms presented in the literature.

Nomenclature

CR	crossover rate	N^{min}	smallest possible value in which the operators can be applied
DV	decision vector	N_m	number of the measured points
F	scaling factor	n, n_1, n_2 , and n_3	ideality factors of the diodes
g	generation number	$P-V$	power–voltage characteristics
G	irradiance (W/m^2)	q	charge of the electron
H	control parameter of LSHADE that represents the number of entries	$RMSE$	root mean square error
$I-V$	current–voltage characteristics	$randc_i$	random integer generated within a specified interval
I_i^{meas} and I_i^{calc}	measured and estimated solar cell currents at point i , respectively	$rand_i$	random number generated from a normal distribution
I_{PV}	photogenerated current	$randn_i$	random number generated from a Cauchy distribution
I_0, I_{01}, I_{02} , and I_{03}	reverse saturation currents	r_i	index selected from range $[1, H]$
K_B	Boltzmann constant	R_P , and R_S	parallel and series resistance of the PV model, respectively
$MAXNFE$	maximum number of fitness evaluations	T	temperature in Kelvin
M_{CR} , and M_F	sets of predefined H -size to store CR_i and F_i values in the memory	V_{th}	thermal voltage
$mean_{WL}(S)$	Lehmer mean of S	W	W solution of Lambert W function
N	population size	x_i	the i th individual in LSHADE algorithm
NFE	current number of fitness evaluations	$\alpha, \beta, \gamma, \delta$, and σ	parameters used in the iterative Lambert W procedure
N^{init}	initial population	ε	accuracy
		θ , and y	variables of the iterative Lambert W procedure

1. Introduction

The growth in solar photovoltaic (PV) power deployment is one of the essential drivers that help decarbonize the energy sector and reduce carbon emissions and greenhouse gases to diminish climate change. Besides, expanding the use of renewable energy, particularly solar PV energy, enables the transition to a green sustainable energy future with reduced conventional non-renewable fossil fuels usage (Mostafa et al., 2020; Abdel Aleem et al., 2015).

To analyze the behavior of a simple solar cell, i.e., to inspect the current–voltage ($I-V$) and power–voltage ($P-V$) characteristics, parameters of the PV equivalent circuit should be precisely estimated while accounting for the physics and main factors driving the behavior of solar PV cells such as irradiance (G) and temperature (T). However, the $I-V$ curve of the solar cell is highly nonlinear in the mathematical sense, making the use of the $I-V$ curve data to generate the parameters inaccurate or produce transcendental equations that are difficult to solve. In that sense, an accurate and reliable parameter estimation method, as well as an adequate equivalent circuit, is required, taking into account the time to estimate the parameters and that the parameters estimated have to match reality and be repeatable to provide similar

measurements for slightly different datasets (Calasan et al., 2020a).

A few equivalent circuits can be found in the literature to appropriately represent solar cells, such as the single diode, double diode, and triple diode models (Calasan et al., 2020a; Bana and Saini, 2016; Nishioka et al., 2007). For PV equivalent circuits, there is a trade-off between simplicity and accuracy. In this regard, the simplest solar cell equivalent circuit model is the single diode model (SDM) (Calasan et al., 2020a; Nishioka et al., 2007). This circuit consists of one DC source (I_{PV}), one diode (connected in parallel with the DC source), in addition to two resistances, connected in parallel (R_P) and series (R_S) with the other elements. The current flowing through the diode can be represented by two parameters (ideality factor (n) and reverse saturation current (I_0)). The SDM has five unknown parameters that should be determined for proper representation of the $I-V$ characteristics. The five parameters are gathered together into a decision vector DV to be adjusted to match the reference characteristics, i.e., $DV = [I_{PV}, I_0, n, R_P, R_S]$. However, SDM cannot take into account all the physical aspects. An overview of the different algorithms used to estimate the PV cell parameters is presented in (Abbassi et al., 2018). Despite the simplicity and ease of implementing the SDM, it has lower accuracy compared to the double diode model (DDM) and triple diode model (TDM). The DDM equivalent circuit comprises two diodes; hence it has seven unknown parameters that

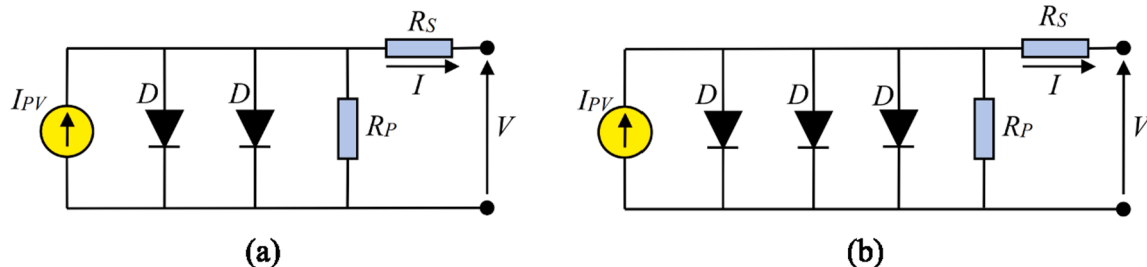


Fig. 1. Solar PV cell equivalent circuits: (a) DDM, and (b) TDM.

Table 1

Results calculated of the conventional and proposed RMSE for double diode parameters estimation of the RTC France solar cell.

No.	Ref.	Algorithm	Original RMSE	RMSE calculated based on (4)	Proposed RMSE calculated using (29)
1	(Yuan et al., 2014)	MPCOA	0.00092163	0.002334758249710	0.001480586318822
2	(Askarzadeh and Rezazadeh, 2013a)	ABSO	0.00098344	0.000983599176727	0.000765494526524
3	(Askarzadeh and Rezazadeh, 2012)	HS	0.00126000	0.001259652017361	0.001053810155791
4		GGHS	0.00107000	0.001068369550208	0.000877968043313
5		IGHS	0.00098635	0.000986572381324	0.000756490370317
6	(El-Naggar et al., 2012)	SA	0.01664000	0.016643532666991	0.010231285515079
7	(Alam et al., 2015)	FPA	0.00078425	0.001242390450280	0.000889429925955
8	(Chen et al., 2018b)	EDDM-LW	NR*	0.001040731340898	0.000770038795066
9	(Jordehi, 2016)	TVAPSO	0.00074365	0.007542232052662	0.004362441851615
10		ICA	0.00085348	0.007117299776128	0.004333741564534
11		TLBO	0.00081280	0.007542334832793	0.004480918763937
12		GWO	0.00090626	0.007618619370821	0.004628221767523
13		WCA	0.00074577	0.007445902613038	0.004363452877615
14		CPSO	0.00074444	0.007454477788164	0.004362534362133
15		PS	0.00816460	0.017260659152888	0.009139402650255
16	(Ram et al., 2017)	BPFPA	0.00072300	0.005697725203041	0.003447871204828
17	(Abd Elaziz and Oliva, 2018)	OBWAO	0.00098251	0.113362521345836	0.075703159839283
18	(Merchaoui et al., 2018)	MPSO	0.00073257	0.275870412266493	0.232410143185828
19	(Chen et al., 2019a)	ISCA	0.00098237	0.000982485156146	0.000757586766079
20	(Yousri et al., 2019)	HCLPSO	0.00074228	0.001231474852965	0.000850623881574
21	(AlHajri et al., 2012)	PS	0.01518000	0.015176662709021	0.010026894375968
22	(Chellaswamy and Ramesh, 2016)	DET	0.00092400	0.006005488061558	0.003447059386445
23	(Xu and Wang, 2017)	GOFPANM	0.00098248	0.000982484856949	0.000757585738047
24	(Rezaee, 2018)	ELPSO	0.00074240	0.007478480168559	0.004360920974088
25		BSA	0.00110851	0.006596785997254	0.004076050928175
26		ABC	0.00080824	0.007256240812734	0.004339331586617
27		GA	0.00591958	0.007254580753415	0.006224119462263
28	(Premkumar et al., 2020)	R-II	0.00098249	0.012157710914671	0.007293813577424
29		R-III	0.00098351	0.011964869016820	0.007220113351526
30		PSO	0.00098602	0.142446620798378	0.077978753325909
31	(Kang et al., 2018)	ImCSA	0.00098249	0.002148064076281	0.001365340427774
32	(Jamadi et al., 2016)	MABC	0.00098276	0.001656860820622	0.001086233371304
33	(Wu et al., 2018)	ABC-TRR	0.00098248	0.000982485799163	0.000757590200733
34		ABC-KP	0.00117240	0.001173156508636	0.000892353209056
35	(Guo et al., 2016)	CSO	0.00098252	0.000982531658369	0.000757760124224
36	(Gong and Cai, 2013)	Rcr-LJADE	0.00098248	0.000982485863500	0.000757590212831
37	(Chen et al., 2016a)	GOTLBO	0.00098318	0.000983151588989	0.000757061996037
38	(Chen et al., 2016b)	EHA-NMS	0.00098248	0.001058219351887	0.000791937012148
39	(Hamid et al., 2016)	NM-MPSO	0.00098250	0.000982716808098	0.000757282698799
40	(Yu et al., 2017a)	SATLBO	0.00098280	0.000982940659354	0.000762457987295
41	(Oliva et al., 2017)	CWOA	0.00098272	0.001157358120869	0.000842359601432
42	(Yu et al., 2017b)	IJAYA	0.00098293	0.001221151800490	0.000984913892457
43		LETBLO	0.00098565	0.000991998756458	0.000774275951105
44		LBSA	0.00098751	0.000999140742904	0.000780352511221
45	(Yu et al., 2019)	PGJAYA	0.00098263	0.000987930649105	0.000756809388952
46		GOTLBO	0.00098742	0.000993727751595	0.000774762028468
47		JAYA	0.00098934	0.000994622635715	0.000781221678366
48		STLBO	0.00098252	0.000982961595179	0.000759274348220
49		TLABC	0.00100120	0.001006063105408	0.000802419976361
50		CLPSO	0.00099894	0.001010017329503	0.000788578621734
51		BLPSO	0.00106280	0.001067287129540	0.000856308638203
52		DE/BBO	0.00102550	0.001025831554119	0.000828355072772
53		CMM-DE/BBO	0.00100880	0.001011159493755	0.000812530939729
54	(Chen et al., 2018a)	TLBO	0.00100692	0.001009281380830	0.000786271261679
55		NIWTLBO	0.00098462	0.000984877007592	0.000768808661519
56		LETBLO	0.00098571	0.000985549690397	0.000773151405993
57		GOTLBO	0.00098544	0.000985404017170	0.000768332426598
58		ABC	0.00098956	0.000989966376687	0.000773971903818
59		GABC	0.00098863	0.000988875282120	0.000778887991163
60		MABC	0.00099203	0.000992375375852	0.000775989911264
61		GBABC	0.00099070	0.000991000963265	0.000759857335540
62		TLABC	0.00098415	0.000984412084666	0.000762846637640
63	(Niu et al., 2014b)	TLBO	0.00099507	0.000992722455528	0.000778960437541
64		STLBO	0.00098248	0.000999255778242	0.000764825710265
65	(Niu et al., 2014a)	BBO-M	0.00098272	0.001050369188820	0.000795135574488
66		BBO	0.00160000	0.003346569820230	0.002172757504432
67		DE	0.00100000	0.001069754810728	0.000810048983135
68	(Oliva et al., 2014)	ABC	0.00098610	0.008763694320310	0.005273399087313
69	(Chen et al., 2019b)	CLPSO	0.00101350	0.001013715375084	0.000813110715151
70		BLPSO	0.00110420	0.001104082585980	0.000915079455519
71		IJAYA	0.00098423	0.000984202126536	0.000761222664494
72		SFS	0.00098255	0.000982570741894	0.000759762500865
73		psFS	0.00098255	0.000982561100518	0.000755741210212
74	(Beigi and Maroosi, 2018)	GA	0.36040000	0.360443905669665	0.359403441378228

(continued on next page)

Table 1 (continued)

No.	Ref.	Algorithm	Original RMSE	RMSE calculated based on (4)	Proposed RMSE calculated using (29)
75		PSO	0.01660000	0.017235132495109	0.010226430997621
76		BFA	0.00120000	0.298267643187141	0.257787612641792
77		FA	0.00101100	0.001011767033445	0.000792728026610
78		HFAPS	0.00098248	0.000982771075757	0.000757676648356
79		ABC	0.00098387	0.001059406511084	0.000788490618975
80	(Lin et al., 2017)	SSO	0.00099129	0.001068039862202	0.000819851009207
81		MSSO	0.00098281	0.001059101400548	0.000794915314275
82	(Askarzadeh and Rezazadeh, 2013b)	BMO	0.00098262	0.000982661460500	0.000754742716132
83	(Mughal et al., 2017)	HPSOSA	0.00074530	0.007459409031783	0.004362786080185
84		CPSO	0.00074530	0.006990871127980	0.004340101765544
85	(Wang et al., 2015)	IABC	0.00100000	0.000994089697903	0.000781769304090
86	(Čalasan et al., 2019)	COA	0.00098248	0.000982484852048	0.000757585390796
87	(Chenouard and El-Sehiemy, 2020)	IBEXOPT-MAE	0.00121800	0.002947029070130	0.001904588431553
88		IBEXOPT-SSE	0.00098457	0.002877090386901	0.001773774791892
89	(Luu and Nguyen, 2020)	MJAYA	0.00098248	0.000983528274794	0.000758013018035
90	(Xiong et al., 2020)	ODE	0.00098252	0.156686903265086	0.089523313619820
91		RTLBO	0.00098252	0.000982521384613	0.000759120697981
92		WLCSODGM	0.00098248	0.000982484852465	0.000757588770141

* NR denotes not reported.

need to be determined and adjusted to match the reference characteristics, i.e., $DV = [I_{PV}, I_{01}, n_1, I_{02}, n_2, R_P, R_S]$. In a physical sense, the DDM considers the combined effect of the junction's neutral region; therefore, it models the solar cells more precisely (Bana and Saini, 2016). The TDM equivalent circuit comprises three diodes; hence it has nine unknown parameters that need to be determined, i.e., $DV = [I_{PV}, I_{01}, n_1, I_{02}, n_2, I_{03}, n_3, R_P, R_S]$. This model was first proposed in (Nishioka et al., 2007) to account for the current leakage through a small-sized solar cell's peripheries. For that reason, TDM is the most accurate solar cell model.

Many methods can be found in the literature for solving the parameter estimation problem of the DDM and TDM. These methods can be broadly categorized into two groups – conventional and metaheuristic methods (Abbassi et al., 2018; Kumar and Kumar, 2017; Ishaque et al., 2011). The conventional methods rely on using analytical solutions or numerical techniques (Kumar and Kumar, 2017). Analytical methods are easy to implement but with less accuracy than the other methods because the simplifications and approximations usually occur to estimate the PV model's unknown parameters. Also, numerical methods rely on using iterative methods such as Newton and Levenberg methods (Ishaque et al., 2011; Elbaset et al., 2014). This set of methods was popular earlier. Currently, the most popular methods are the methods based on evolutionary algorithms (EAs) that use the power of metaheuristics in solving the PV parameters estimation problem (Yuan et al., 2014; Abbassi et al., 2018; Zobaa et al., 2018). Examples of EAs used to solve this problem are swarming-based algorithms as ABSO (Askarzadeh and Rezazadeh, 2013a), TVACPSO (Jordehi, 2016), BPFPA (Ram et al., 2017), MPSO (Merchaoui et al., 2018), ELPSO (Rezaee, 2018), MABC (Jamadi et al., 2016), ABC-KP (Wu et al., 2018), ABC-TRR (Wu et al., 2018), BLPSO (Yu et al., 2019), ABC (Chen et al., 2018a), GABC (Chen et al., 2018a), GBABC (Chen et al., 2018a), BFA (Beigi and Maroosi, 2018), MSSO (Lin et al., 2017), and BMO (Askarzadeh and Rezazadeh, 2013b), bio inspiration-based algorithms as DET (Chellawamy and Ramesh, 2016), GA (Rezaee, 2018), DE/BBO (Yu et al., 2019), and DE (Niu et al., 2014a), physics and chemistry-based algorithms as HS (Askarzadeh and Rezazadeh, 2012), IGHS (Askarzadeh and Rezazadeh, 2012), GGHS (Askarzadeh and Rezazadeh, 2012), SA (El-

Naggar et al., 2012), WCA (Jordehi, 2016), BBO (Niu et al., 2014a), and BBO-M (Niu et al., 2014a), teaching and learning process-based algorithms as TLO (Premkumar et al., 2020), LBSA (Yu et al., 2017b), CLPSO (Yu et al., 2019), TLABC (Chen et al., 2018a), NIWTLBO (Chen et al., 2018a), LETLBO (Chen et al., 2018a), STLBO (Niu et al., 2014b), and TLBO (Niu et al., 2014b), and chaotic behavior-based algorithms as MPCOA (Yuan et al., 2014), CPSO (Jordehi, 2016), CWOA (Oliva et al., 2017), and COA (Čalasan et al., 2019). Besides, some researchers used hybrid conventional and metaheuristic methods to combine the best of both categories – the simplicity of the conventional methods and effectiveness of the metaheuristic methods. Examples are EHA-NMS (Chen et al., 2016b), DE/BBO (Yu et al., 2019), HFAPS (Beigi and Maroosi, 2018), and HPSOSA (Mughal et al., 2017). The reader can refer to (Abbassi et al., 2018; Baig et al., 2020) for more details on the formulation of these methods and their applications.

In general, the more complex the PV model, the more difficult it is to formulate and find its parameters. In this regard, the calculation of RMSE between measured and estimated solar cell characteristics is one of the main criteria used in obtaining the solutions to the parameter estimation problem of the solar PV equivalent circuits. An approximated expression for the calculated solar cell current is usually used in parameters estimation of solar cell models in the literature. Accordingly, in the mathematical sense, the RMSE is not correctly calculated. In this regard, Čalasan et al. (2020a) have derived an analytical solution for solar cell current and root-mean-square error (RMSE) calculations to solve the 5-parameter estimation problem of the SDM of PV cells. Also, Peng et al. (2013) presented an improved photovoltaic cell model using the Lambert W function. The PV cell's I - V and P - V curves were calculated and simulated in Matlab/Simulink environment. The method introduced shows good agreement between the I - V points. It was found that the proposed modeling method has less error at the maximum power point state. Besides, Wu and Peng (2018) presented a maximum power point detection method for the PV module based on Lambert W function to achieve high-precision detection while obtaining the maximum power point solution. Chen et al. (2018b) presented an explicit double-diode model based on the Lambert W function by

Table 2

Results calculated of the conventional and proposed RMSE for double diode parameters estimation of the Solarex MSX-60 module.

No.	Ref.	Algorithm	RMSE calculated based on (4)	Proposed RMSE calculated using (29)
1	(Kumar and Kumar, 2017)	Analytical	0.034413714142117	0.025616610413287
2		Numerical	0.049134195943897	0.030629821992676
3	(Ishaque et al., 2011)	Iteration method	0.147217689512839	0.078175204490548
4	(Elbaset et al., 2014)	Newton method	0.194975315385194	0.101859948842175
5	(Čalasan et al., 2019)	COA	0.019594472976615	0.013663131531381

Table 3

Results calculated of the conventional and proposed RMSE for triple diode parameters estimation of the RTC France solar cell.

No.	Ref.	Algorithm	Original RMSE	RMSE calculated based on (5)	Proposed RMSE calculated using (29)
1	(Premkumar et al., 2020)	R-II	0.000980467	0.008587146230420	0.005107411023299
2		R-III	0.000980443	0.003681070948844	0.002249998268702
3		PSO	0.000986907	0.003502047703695	0.002171714157475
4		CS	0.000987857	0.007644977536513	0.004569170371860
5		ABC	0.000982276	0.004084742194699	0.002471743406221
6		TLO	0.000981541	0.001024435157923	0.000779584031444
7	(Abd Elaziz and Oliva, 2018)	ABC	0.000984660	0.001455032241954	0.000990246961966
8		OBWOA	0.000982490	0.001121702913461	0.000823136021013
9		STLBO	0.000982530	0.001123061802693	0.000823698446910

defining two new parameters to separate the exponential function in DDM to use the Lambert W function. However, no exact analytical solution has been reached for the current expressions of the DDM and TDM, with no additional parameters, because of the high nonlinearity of these models' current expressions.

None of the optimization algorithms presented in the literature has yet proved its superiority in RMSE calculation. In this work, a novel iterative procedure based on the Lambert W function is proposed to redress this gap in this work for the analysis of the solar cell current in both DDM and TDM. The RMSE values calculated using the parameters found by many optimization algorithms presented in the literature are presented and discussed for the RTC France PV cell and Solarex MSX-60 PV module. The results obtained show that RMSE values were not accurately calculated in most of the methods presented in the literature. Further, an improved LSHADE optimization algorithm called Chaotic LSHADE (CLSHADE) algorithm is proposed to solve the 7-parameter and 9-parameter estimation problem of the PV equivalent circuits. The proposed methodology is also applied to $I-V$ characteristics measured in the laboratory for solar modules of Clean Energy Trainer Setup (CETS). The 7 and 9 unknown parameters are estimated using the CLSHADE algorithm based on minimizing the RMSE values.

The article is divided into several sections. Section 2 provides necessary information about the DDM and TDM equivalent circuits. The conventional methodology used for calculation of the solar cell current of both models is presented. Further, the iterative procedure proposed for analyzing the solar cell current in both DDM and TDM is explored. Besides, the proposed RMSE expression for both models is formulated. Section 3 gives the results of parameter estimation and RMSE values calculated of the DDM and TDM equivalent circuits compared to the literature results. Section 4 presents the improved CLSHADE algorithm proposed in this work. Section 5 presents the results of the optimization problem. Furthermore, the experimental validations of the proposed algorithm and the corresponding simulation results are given. Finally, the conclusions drawn out from work are presented in Section 6.

2. Solar cell current and proposed RMSE calculations of DDM and TDM

The DDM and TDM equivalent circuits are shown in Fig. 1.

The $I-V$ relationship of the DDM and TDM solar cell equivalent circuits is represented, respectively, as follows:

$$I = I_{PV} - I_{01} \left(e^{\frac{V+IR_S}{n_1 V_{th}}} - 1 \right) - I_{02} \left(e^{\frac{V+IR_S}{n_2 V_{th}}} - 1 \right) - \frac{V + IR_S}{R_P} \quad (1)$$

$$I = I_{PV} - I_{01} \left(e^{\frac{V+IR_S}{n_1 V_{th}}} - 1 \right) - I_{02} \left(e^{\frac{V+IR_S}{n_2 V_{th}}} - 1 \right) - I_{03} \left(e^{\frac{V+IR_S}{n_3 V_{th}}} - 1 \right) - \frac{V + IR_S}{R_P} \quad (2)$$

where I_{PV} denotes the photogenerated current, I_{01} , I_{02} , and I_{03} denote the reverse saturation current of the three diodes, respectively, n_1 , n_2 , and n_3 represent the ideality factors of the three diodes, and $V_{th} = K_B T/q$ is the thermal voltage (K_B is Boltzmann constant, T is the temperature in

Kelvin and q is the charge of the electron).

2.1. Conventional solar cell current calculations of DDM and TDM

In line with the literature, for the solar PV equivalent circuits, (3) is usually used for RMSE calculation.

$$RMSE = \sqrt{\frac{1}{N_m} \sum_{i=1}^{N_m} (I_i^{meas} - I_i^{calc})^2} \quad (3)$$

where N_m represents the number of the measured points, while I_i^{meas} and I_i^{calc} represent the measured and estimated solar cell currents at the i th point, respectively, where $i \in N_m$.

For $V^{calc} = V^{meas}$, the solar cell current expressions in the DDM and TDM circuits are commonly expressed in (4) and (5), respectively, as follows:

$$I_i^{calc} = I_{PV} - I_{01} \left(e^{\frac{V_i^{meas} + I_i^{meas} R_S}{n_1 V_{th}}} - 1 \right) - I_{02} \left(e^{\frac{V_i^{meas} + I_i^{meas} R_S}{n_2 V_{th}}} - 1 \right) - \frac{V_i^{meas} + I_i^{meas} R_S}{R_P} \quad (4)$$

$$I_i^{calc} = I_{PV} - I_{01} \left(e^{\frac{V_i^{meas} + I_i^{meas} R_S}{n_1 V_{th}}} - 1 \right) - I_{02} \left(e^{\frac{V_i^{meas} + I_i^{meas} R_S}{n_2 V_{th}}} - 1 \right) - I_{03} \left(e^{\frac{V_i^{meas} + I_i^{meas} R_S}{n_3 V_{th}}} - 1 \right) - \frac{V_i^{meas} + I_i^{meas} R_S}{R_P} \quad (5)$$

However, the used expressions for the calculated values of the solar cell currents are not mathematically correct because both the measured solar cell current and voltage are used in the current calculation. In other words, the last terms in (4) and (5) do not reflect the correct calculated value of the solar cell output current. Therefore, pseudo-substituting (4) or (5) into (3) will not result in a valid RMSE expression for the DDM and TDM equivalent circuits.

Table 4

Results calculated of the conventional and proposed RMSE for triple diode parameters estimation of the Solarex MSX-60 module.

No.	Ref.	Algorithm	RMSE calculated based on (5)	Proposed RMSE calculated using (29)
1	(Elazab et al., 2020)	GA	0.475095170477594	0.330611770090420
2		SA	0.118271885724707	0.104893994226613
3		WOA	0.241434077910324	0.189198965224155
4	(Qais et al., 2019a)	SFO	0.033171485486887	0.025094707623453
5		GA	0.616907358890717	0.483098697415653
6		SA	1.261419033964690	1.092819646922040
7		WOA	0.592760429128359	0.450792347716254
8	(Qais et al., 2019b)	COOA	0.326509126223926	0.255922197819495

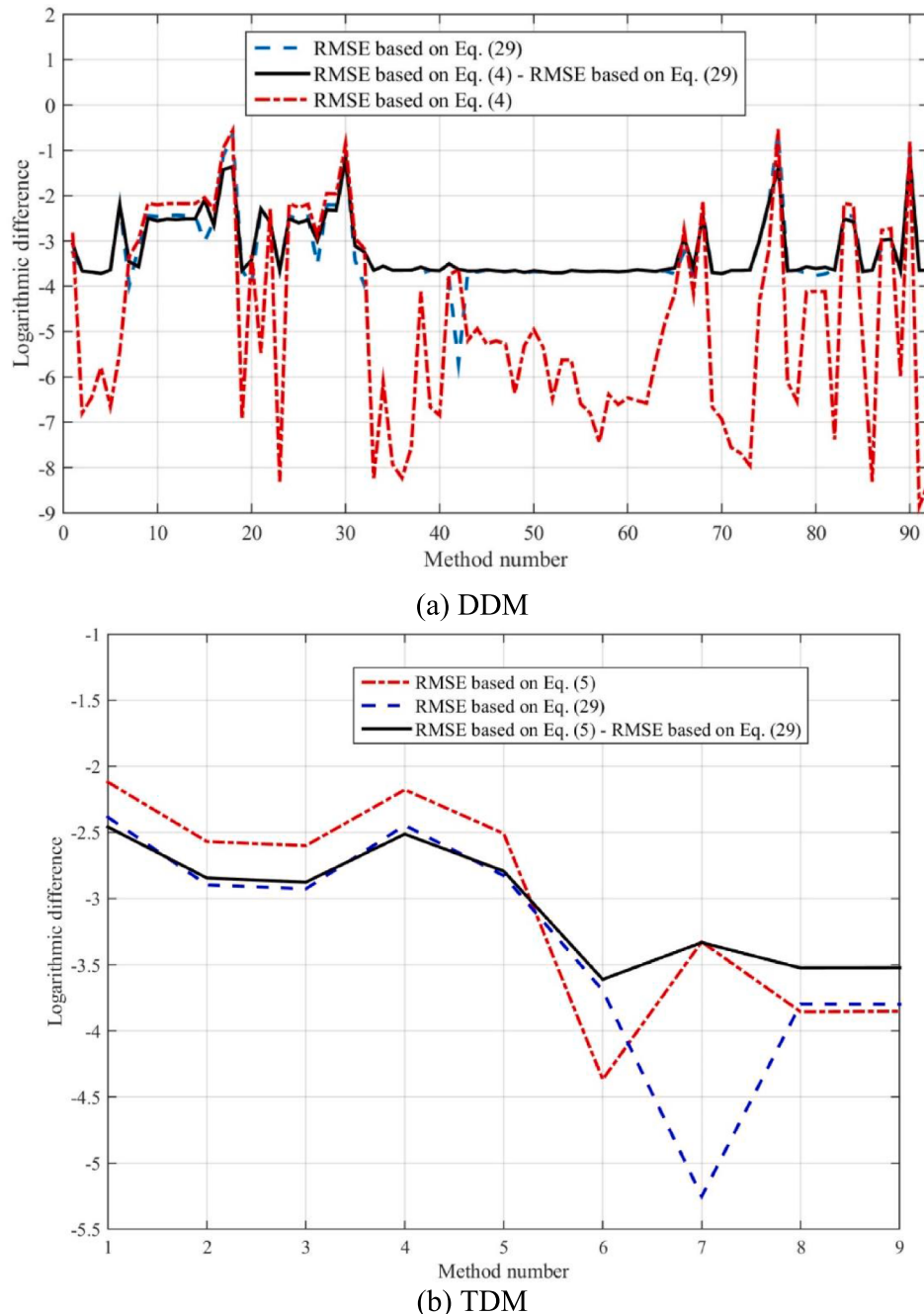


Fig. 2. Difference between RMSE values calculated for the RTC cell: (a) DDM, (b) TDM.

2.2. Proposed iterative procedure for solar cell current calculations of DDM and TDM

2.2.1. Solar cell current calculation for the DDM equivalent circuit

For the DDM, (4) can be formulated as follows:

$$\alpha + \beta e^{\delta y} = y e^y \quad (6)$$

where

$$\alpha = \frac{\frac{R_S}{n_1 V_{th}}}{\left(1 + \frac{R_S}{R_P}\right)} I_{01} \left(\exp\left(\frac{V}{n_1 V_{th}}\right) \right) \exp\left(\frac{\frac{R_S}{n_1 V_{th}} \left(I_{PV} + I_{01} + I_{02} - \frac{V}{R_P} \right)}{\left(1 + \frac{R_S}{R_P}\right)}\right) \quad (7)$$

$$\beta = \frac{\frac{R_S}{n_1 V_{th}}}{\left(1 + \frac{R_S}{R_P}\right)} I_{02} \exp\left(\frac{V}{n_2 V_{th}}\right) \exp\left(\frac{R_S}{n_2 V_{th}} \frac{\left(I_{PV} + I_{01} + I_{02} - \frac{V}{R_P} \right)}{\left(1 + \frac{R_S}{R_P}\right)}\right) \quad (8)$$

$$\delta = 1 - \frac{n_1}{n_2} \quad (9)$$

Based on (6), the current expression presented in (4) can be rewritten as follows:

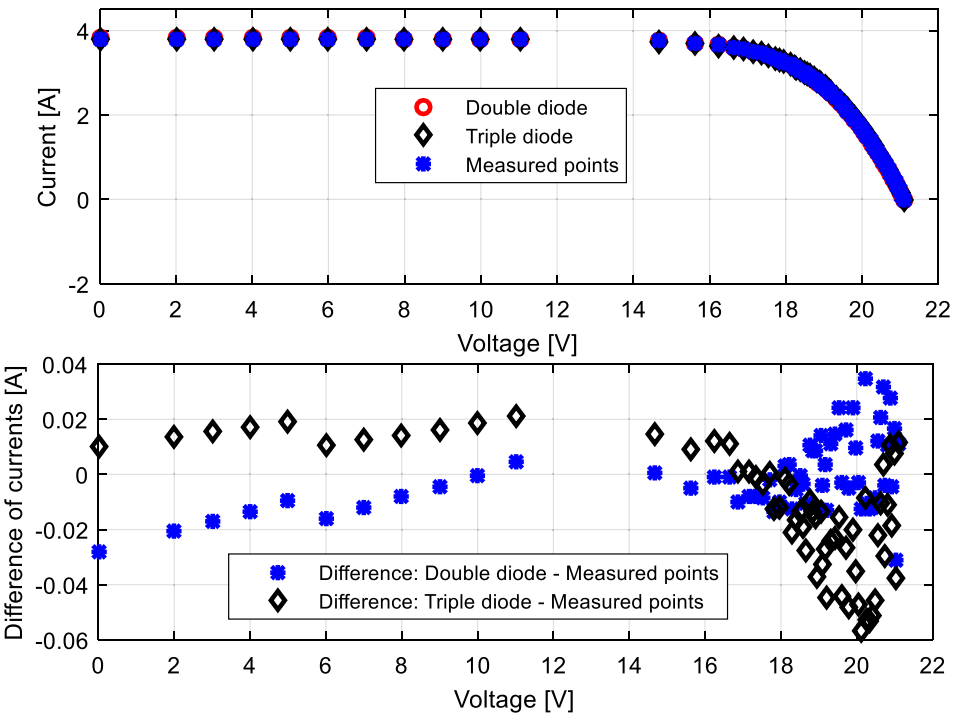


Fig. 3. I-V characteristics of the Solarex MSX-60 PV module and the differences between the estimated and measured characteristics.

$$I = \frac{I_{PV} + I_{01} + I_{02} - \frac{V}{R_P} - \frac{y \left(1 + \frac{R_S}{R_P} \right)}{\frac{R_S}{n_1 V_{th}}}}{1 + \frac{R_S}{R_P}} \quad (10)$$

Equation (10) is a transcendental equation that cannot be solved analytically. Hence, the following iterative procedure is proposed to solve it.

The iteration procedure starts with an initial value of the variable y denoted as $y_{(0)}$. Then, the initial value of the parameter θ denoted as $\theta_{(0)}$ is calculated as follows:

$$\theta_{(0)} = \alpha + \beta \exp(\delta y_{(0)}) \quad (11)$$

Then, we need to update the value of y in the first iteration, thus;

$$\theta_{(0)} = y_{(1)} \exp y_{(1)} \quad (12)$$

Equation (12) is a well-known Lambert W equation ([Calasan and Nedic, 2018; Čalasan, 2019; Čalasan et al., 2020a](#)). Therefore, it can be easily solved, as follows:

$$y_{(1)} = W(\theta_{(0)}) \quad (13)$$

where W is the solution of the Lambert W equation. Accordingly, one can get the updated θ value, denoted as $\theta_{(1)}$, as follows:

$$\theta_{(1)} = \alpha + \beta \exp(\delta y_{(1)}) \quad (14)$$

Then, we need to check the absolute value of the difference between current and updated θ values, as follows:

$$\epsilon = |\theta_{(1)} - \theta_{(0)}| \quad (15)$$

where ϵ is an arbitrary small number (i.e., $\epsilon = 10^{-15}$). If the error criterion represented by (15) does not satisfy the predefined limit, the initial value $y_{(0)}$ is changed to $y_{(1)}$ in the iteration comes next, and the whole procedure is repeated until the error criterion is satisfied. Therefore, for the p th iteration, one can write $y_{(p)}$ as follows:

$$y_{(p)} = W\left(\alpha + \beta \exp(\delta y_{(p-1)})\right) \quad (16)$$

To that end, using the proposed iterative procedure, one can formulate the p th double diode solar cell current expression as follows:

$$I_{(p)} = \frac{I_{PV} + I_{01} + I_{02} - \frac{V}{R_P} - \frac{y_{(p)} \left(1 + \frac{R_S}{R_P} \right)}{\frac{R_S}{n_1 V_{th}}}}{1 + \frac{R_S}{R_P}} \quad (17)$$

For more clarity for the reader, the Matlab code used for solving (11) using the iterative Lambert W equation is given in Appendix 1. Furthermore, numerical examples of solving the iterative Lambert W of the DDM's equation are given in Appendix 2.

2.2.2. Solar cell current calculation for the TDM equivalent circuit

In the same way, for the TDM, (5) can be formulated as follows:

$$\alpha + \beta e^{\delta y} + \gamma e^{\sigma y} = y e^y \quad (18)$$

where

$$\alpha = \frac{\frac{R_S}{n_1 V_{th}}}{\left(1 + \frac{R_S}{R_P} \right)} I_{01} \exp\left(\frac{V}{n_1 V_{th}}\right) \exp\left(\frac{\frac{R_S}{n_1 V_{th}} \left(I_{PV} + I_{01} + I_{02} + I_{03} - \frac{V}{R_P} \right)}{\left(1 + \frac{R_S}{R_P} \right)}\right) \quad (19)$$

$$\beta = \frac{\frac{R_S}{n_1 V_{th}}}{\left(1 + \frac{R_S}{R_P} \right)} I_{02} \exp\left(\frac{V}{n_2 V_{th}}\right) \exp\left(\frac{\frac{R_S}{n_2 V_{th}} \left(I_{PV} + I_{01} + I_{02} + I_{03} - \frac{V}{R_P} \right)}{\left(1 + \frac{R_S}{R_P} \right)}\right) \quad (20)$$

$$\gamma = \frac{\frac{R_S}{n_1 V_{th}}}{\left(1 + \frac{R_S}{R_P} \right)} I_{03} \exp\left(\frac{V}{n_3 V_{th}}\right) \exp\left(\frac{\frac{R_S}{n_3 V_{th}} \left(I_{PV} + I_{01} + I_{02} + I_{03} - \frac{V}{R_P} \right)}{\left(1 + \frac{R_S}{R_P} \right)}\right) \quad (21)$$

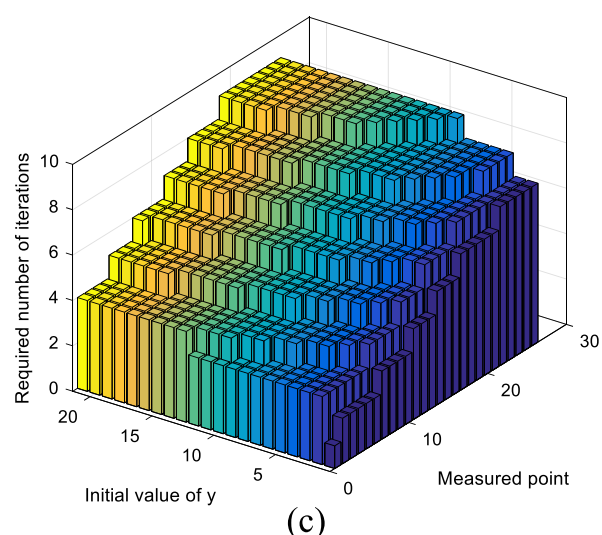
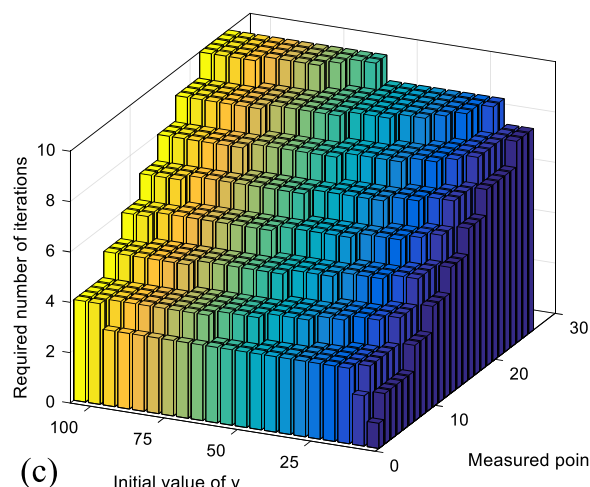
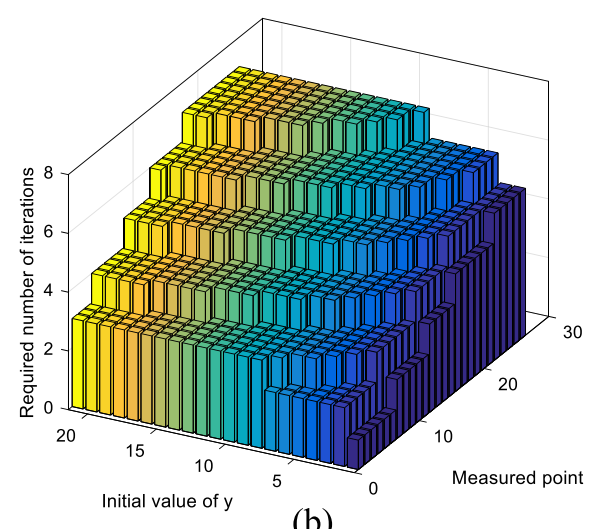
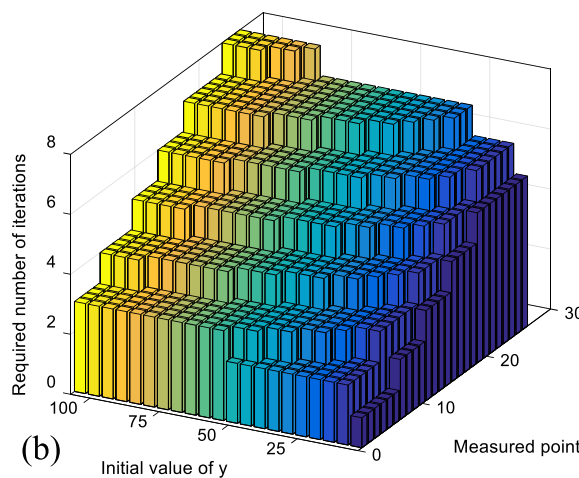
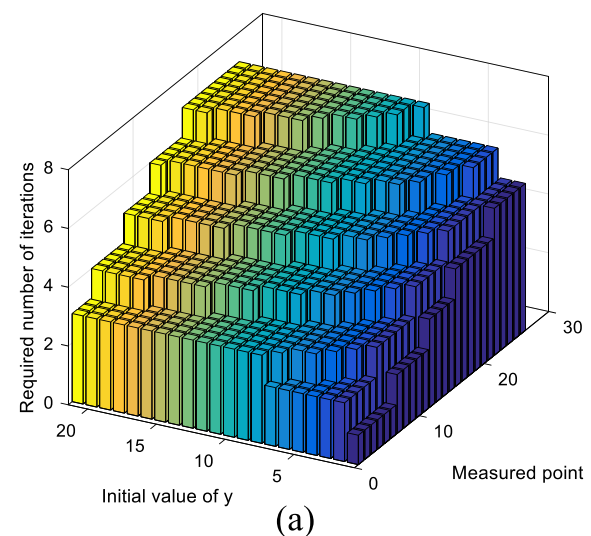
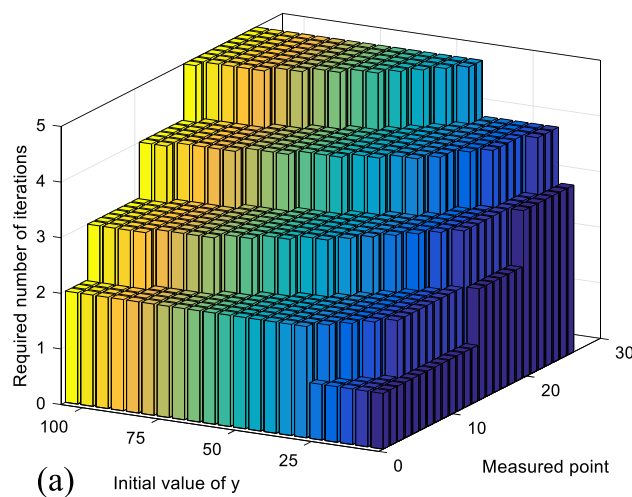


Fig. 4. Required number of iterations versus different initial values and accuracy values (RTC France solar cell, DDM of the solar cell): (a) $\epsilon = 10^{-5}$, (b) $\epsilon = 10^{-10}$ and (c) $\epsilon = 10^{-15}$

Fig. 5. Required number of iterations versus different initial values and accuracy values (RTC France solar cell, TDM of the solar cell): (a) $\epsilon = 10^{-5}$, (b) $\epsilon = 10^{-10}$ and (c) $\epsilon = 10^{-15}$

$$\delta = 1 - \frac{n_1}{n_2} \quad (22)$$

$$\sigma = 1 - \frac{n_1}{n_3} \quad (23)$$

In this case, the triple diode solar cell current is formulated as follows:

$$I = \frac{I_{PV} + I_{01} + I_{02} + I_{03} - \frac{V}{R_P} - \frac{y \left(1 + \frac{R_S}{R_P} \right)}{\frac{R_S}{n_1 V_{th}}}}{1 + \frac{R_S}{R_P}} \quad (24)$$

Equation (24) is a transcendental equation that cannot be solved analytically. Hence, the following iterative procedure is proposed to solve it.

The iteration procedure starts with $y_{(0)}$. Then, $\theta_{(0)}$ is calculated as follows:

$$\theta_{(0)} = \alpha + \beta \exp(\delta y_{(0)}) + \gamma \exp(\sigma y_{(0)}) \quad (25)$$

Then, we need to update the value of y in the first iteration, thus;

$$\theta_{(0)} = y_{(1)} \exp y_{(1)} \quad (26)$$

Equation (26) is a well-known Lambert W equation. Therefore, it can be easily solved, as explained before. Thus, for the p th iteration, one can write $y_{(p)}$ as follows:

$$y_{(p)} = W\left(\alpha + \beta \exp(\delta y_{(p-1)}) + \gamma \exp(\sigma y_{(p-1)})\right) \quad (27)$$

Hence, one can formulate the p th triple diode solar cell current expression as follows:

$$I_{(p)} = \frac{I_{PV} + I_{01} + I_{02} + I_{03} - \frac{V}{R_P} - \frac{y_{(p)} \left(1 + \frac{R_S}{R_P} \right)}{\frac{R_S}{n_1 V_{th}}}}{1 + \frac{R_S}{R_P}} \quad (28)$$

For more clarity for the reader, numerical examples of solving the iterative Lambert W of the TDM's equation are given in Appendix 2.

2.2.3. RMSE calculation for DDM and TDM equivalent circuits

Unlike most papers that use Eqs. (4) and (5) for the RMSE calculation for DDM and TDM equivalent circuits, in this work, the following expression based on the iterative procedure of the Lambert W equation has proposed for PV parameters estimation of DDM and TDM equivalent circuits.

$$RMSE = \sqrt{\frac{1}{N_m} \sum_{i=1}^{N_m} \left(I_i^{meas} - I_{i,(p)}^{calc} \right)^2} \quad (29)$$

where $I_{i,(p)}^{calc}$ denotes the p th solar cell current at point i , in which $I_{i,(p)}^{calc}$ is expressed in (17) for the DDM and in (28) for the TDM.

3. Numerical results and discussion

In Table 1, for the RTC France solar cell, the RMSE values calculated based on 92 different methods explored in many papers are presented for the double diode solar cell parameters. Also, the RMSE values calculated based on (4), and the corrected RMSE values computed using (29) are presented. Moreover, in Table 2, the same data for the Solarex MSX-60 PV module are presented. Similarly, for the TDM, Tables 3 and 4 show the corresponding data for both RTC France solar cell and Solarex MSX-60 PV module, respectively. The calculations are carried out on a personal computer, Intel (R) Core (TM) i3-7020U CPU, 2.30 GHz, and 4 GB RAM using the Matlab program. The Lambert W equation embedded in Matlab was used, with accuracy equals 10^{-15} for all points,

Table 5

Pseudo-code shows the memory update procedure.

Algorithm 1: Memory update

```
If  $S_{CR} \neq \emptyset$  and  $S_F \neq \emptyset$  then
    if  $M_{CR,k,g} = \perp$  or  $\max(S_{CR}) = 0$ , then
         $M_{CR,k,g+1} = \perp$ ;
    Else
         $M_{CR,k,g+1} = \text{mean}_{WL}(S_{CR})$ ;
         $M_{F,k,g+1} = \text{mean}_{WL}(S_F)$ ;
         $k += 1$ ;
        If  $k > H$ ,
             $k = 1$ ;
        else
             $M_{CR,k,g+1} = M_{CR,k,g}$ ;
             $M_{F,k,g+1} = M_{F,k,g}$ ;
    end
```

Table 6

Pseudo-code shows the LSHADE algorithm.

Algorithm 2: LSHADE algorithm

```
// Initialization phase
→  $g = 1$ ,  $Ng = N^{init}$ , Archive A =  $\emptyset$ ;
→ Initialize population randomly;
→ Set all values in  $M_{CR}$ ,  $M_F$  to 0.5;
// Main loop
→ while the termination criterion is not met do
     $S_{CR} = \emptyset$ ,  $S_F = \emptyset$ ;
    for  $i = 1$  to N do
         $r_i = \text{select from } [1, H] \text{ randomly}$ ;
        If  $M_{CR,ri} = \perp$ ,  $CR_{i,g} = 0$ . Otherwise
             $CR_{i,g} = \text{randni}(M_{CR,ri}, 0.1)$ ;
             $F_{i,g} = \text{randci}(M_F,ri, 0.1)$ ;
            Generate trial vector  $u_{i,g}$  according to current-to-best/1/bin;
        for  $i = 1$  to N do
            if  $f(u_{i,g}) \leq f(x_{i,g})$  then
                 $x_{i,g+1} = u_{i,g}$ ;
            else
                 $x_{i,g+1} = x_{i,g}$ ;
                if  $f(u_{i,g}) < f(x_{i,g})$  then
                     $x_{i,g} \rightarrow A$ ;
                     $CR_{i,g} \rightarrow S_{CR}$ ,  $F_{i,g} \rightarrow S_F$ ;
    If necessary, delete randomly selected individuals from the archive such that the
    archive size is  $|A|$ .
    // Optional LPSR strategy
    Calculate  $N_{g+1}$ 
    if  $Ng < N_{g+1}$  then
        Sort individuals in the population based on their fitness values and delete
        lowest  $N_g - N_{g+1}$  members;
        Resize archive size  $|A|$  according to the new population;
    →  $g++$ ;
```

for the iterative procedure. The double diode and triple diode solar cell parameters' values using the different methods addressed in Tables 1–4 are given in Appendix 3, respectively.

In Tables 1–4, there are differences observed between the calculated RMSE values and the original RMSE values presented in the papers. This can occur for many reasons, such as using a few or a certain number of points in the I – V characteristics or compact values of the physical factors or parameters (Calasan et al., 2020a).

Based on the results obtained, the RMSE values were not accurately calculated in most of the presented methods, in which the difference between the original RMSE values calculated for all the considered methods is illustrated in Fig. 2 for the RTC France solar cell results obtained based on (4) and (29) for the DDM and (5) and (29) for the TDM.

The I – V characteristic of the Solarex MSX-60 PV module obtained for these parameters and the measured characteristics are explored in Fig. 3, in which the difference between the estimated and measured characteristics are presented in the same figure.

The impact of the initial value of variable y on the iterative procedure and the effect of the number of the measured points on the

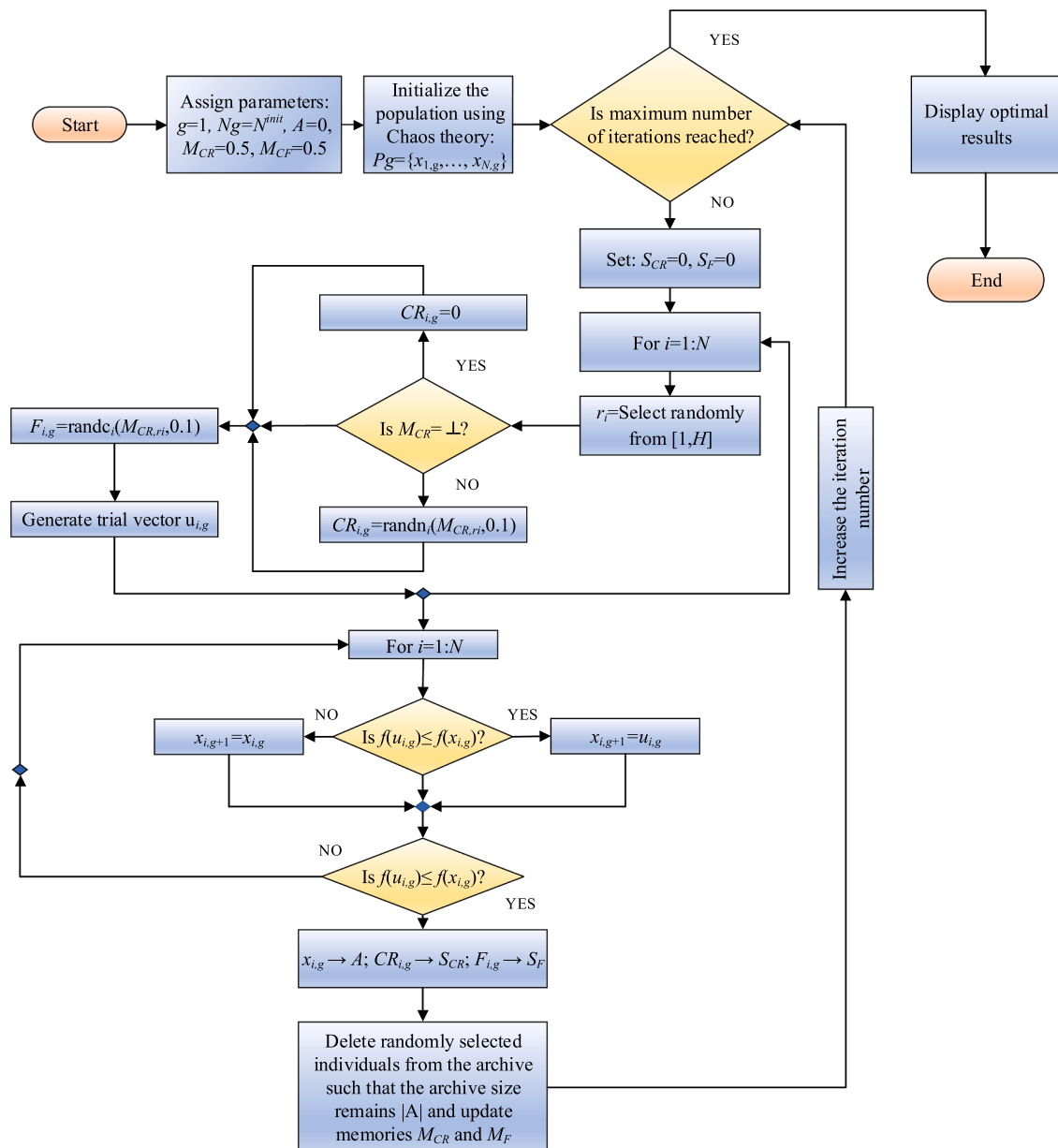


Fig. 6. Flow chart of the CLSHADE algorithm.

required number of iterations are presented in Fig. 4 for the DDM and Fig. 5 for the TDM. This test is performed using three accuracy values: $\epsilon = 10^{-5}$, 10^{-10} , and 10^{-15} . In this case, the RTC France solar cell parameters were determined using the BMO method for the DDM and the TLO method for the TDM (i.e., results of method 82 for the DDM – Table 1, and method 6 for the TDM – Table 3). From both figures, it is evident that the proposed iterative procedure is very efficient. A permissible accuracy value can be obtained after a few iterations for some measured points and a small number of initial values. For $\epsilon = 10^{-15}$, the proposed iterative procedure does not require a significantly higher number of iterations compared to the other cases. Besides, it is justified to use a smaller initial value of variable y . To conclude, the accuracy of optimization techniques relies on RMSE calculation can be improved by using the proposed solar cell current expressions and the RMSE calculated based on them, as presented in the following sections.

4. Chaotic LSHADE

Differential evolution (DE) represents one of the most commonly used EAs. SHADE (Success-history based adaptive DE) belongs to the DE algorithms, in which a mechanism is applied for parameter adaptation based on the historical memory of successful parameter settings that were determined during previous runs (Tanabe and Fukunaga, 2013). In the literature, an upgraded version of the SHADE algorithm known as the LSHADE algorithm is presented (Tanabe and Fukunaga, 2013; Tanabe and Fukunaga, 2014), in which a continuous linear population size reduction methodology (LPSR), reduction of the population size is applied.

In a mathematical sense, the population size (N) in the next generation ($g + 1$), denoted as N_{g+1} , can be written as follows:

$$N_{g+1} = \text{round} \left[\left(\frac{N^{\min} - N^{\max}}{\text{MAXNFE}} \right) N\text{FE} + N^{\max} \right] \quad (30)$$

Table 7

Boundaries for DDM and TDM parameters for the RTC France solar cell and Solarex MSX-60 PV module.

Variables	RTC France solar cell				Solarex MSX-60 PV module			
	DDM		TDM		DDM		TDM	
	LB	UB	LB	UB	LB	UB	LB	UB
I_{PV} (A)	0.0	1.0	0.0	1.0	3.5	4.0	3.5	4.0
I_{01} (μ A)	0.0	1.0	0.0	1.0	10×10^{-4}	1.0	10×10^{-4}	1.0
I_{02} (μ A)	0.0	1.0	0.0	1.0	10×10^{-4}	1.0	0.0	1.0
I_{03} (μ A)	–	–	0.0	1.0	–	–	10×10^{-4}	1.0
R_S (Ω)	0.0	0.5	0.0	0.5	0.2	0.4	0.2	0.4
R_P (Ω)	0.0	100.0	0.0	100.0	150.0	3000.0	150.0	3000.0
n_1	1.0	2.0	1.0	2.0	1.0	2.0	1.0	2.0
n_2	1.0	2.0	1.0	2.0	1.0	2.0	1.0	2.0
n_3	–	–	1.0	2.0	–	–	1.0	2.0

where N^{min} is set to the smallest possible value such that the evolutionary operators can be applied, NFE is the current number of fitness evaluations, $MAXNFE$ is the maximum number of fitness evaluations, and g denotes the generation number (Calasan et al., 2020b).

For each particular generation g , the specific-individual adaptive control parameters CR_i (CR is the crossover rate) and F_i (scaling factor) used by each individual (x_i) are generated by selecting the index r_i from $[1, H]$ randomly, where H is a control parameter of the LSHADE algorithm that represents the number of entries. These parameters are expressed as follows:

$$r_i = randi(1, H) \quad (31)$$

$$CR_i = \begin{cases} 0 & \text{if } M_{CR_i} = \perp \\ randn_i(M_{CR_i}, 0.1) & \text{Otherwise} \end{cases} \quad (32)$$

$$F_i = randc_i(M_{F_i}, 0.1) \quad (33)$$

where $rand_i$, $randn_i$, and $randc_i$ are random integer generated within a specified interval, a random number generated from a normal distribution, and a random number generated from a Cauchy distribution. M_{CR_i} and M_{F_i} are sets of predefined H -size to store in memory CR_i and F_i values, and the associated information, that have performed well in the past generations.

Further, a mutant vector $v_{i,g}$ is generated from the existing population members as follows:

$$v_{i,g} = x_{i,g} + F_i(x_{pbest,g} - x_{i,g}) + F_i(x_{r_1,g} - x_{r_2,g}) \quad (34)$$

Where $x_{pbest,g}$ is the best individual in the current generation. The subscripts r_1, r_2 are randomly selected from $[1, N]$, so that $r_1 \neq r_2$.

For each dimension j , if the mutant vector element $v_{j,i,g}$ failed to satisfy the predefined limits $[x_j^{min} \ x_j^{max}]$, the corrective formula, given in (35), is performed as follows:

$$v_{j,i,g} = \begin{cases} \frac{x_j^{min} + x_{j,i,g}}{2} & \text{if } v_{j,i,g} \leq x_j^{min} \\ \frac{x_j^{max} + x_{j,i,g}}{2} & \text{if } v_{j,i,g} \geq x_j^{max} \end{cases} \quad (35)$$

The crossover function is defined based on the crossover probability of assignment as follows:

$$u_{j,i,g} = \begin{cases} v_{j,i,g} & \text{if } rand(0, 1) \leq CR_i \\ x_{j,i,g} & \text{otherwise} \end{cases} \quad (36)$$

After all of the trial vectors have been generated, the next step is the selection process to determine the next generation's survivors.

$$x_{i,g+1} = \begin{cases} u_{i,g} & \text{if } f(u_{i,g}) \leq f(x_{i,g}) \\ x_{i,g} & \text{otherwise} \end{cases} \quad (37)$$

Table 8

Optimal DDM and TDM parameters for the RTC France solar cell and Solarex MSX-60 PV module.

Variables	RTC France solar cell		Solarex MSX-60 module	
	DDM	TDM	DDM	TDM
I_{PV} (A)	0.76076	0.76076	3.812527	3.81253
I_{01} (μ A)	0.20440	0.87650	0.12311	0.12311
I_{02} (μ A)	8.76400×10^{-1}	2.04400×10^{-1}	7.29990×10^{-5}	7.29985×10^{-5}
I_{03} (μ A)	–	0.000180	–	0.000125
R_S (Ω)	0.036907	0.036920	0.226800	0.226760
R_P (Ω)	55.53000	55.68000	800.00000	823.40000
n_1	1.44241	1.99500	1.32290	1.32270
n_2	1.99520	1.44240	1.98800	1.99000
n_3	–	1.89000	–	1.93000
Conventional RMSE	0.000985014	0.000984015	0.017574595	0.017009787
Proposed RMSE	0.000752742	0.000751850	0.012029276	0.011653038

In each generation, CR_i and F_i are recorded as S_{CR} , S_F and at the end of the generation, the memory contents are updated using the algorithm shown in Table 5.

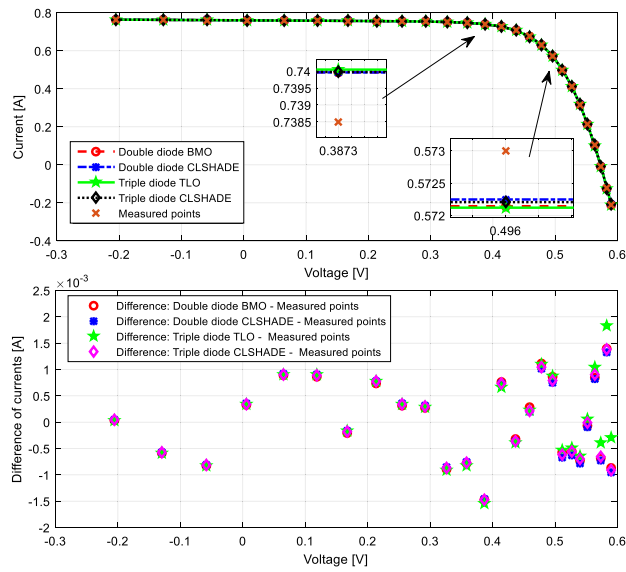
In this algorithm, the index k determines the position in the memory to update. k is initialized at 1 at the beginning of the search, and it is increased when a new element is inserted into history. When all individuals in generation g fail to generate a better trial vector than the parent, the memory is not updated.

This part of the LSHADE algorithm also contains the calculation of Lehmer mean denoted $mean_{WL}(S)$. It is computed as follows:

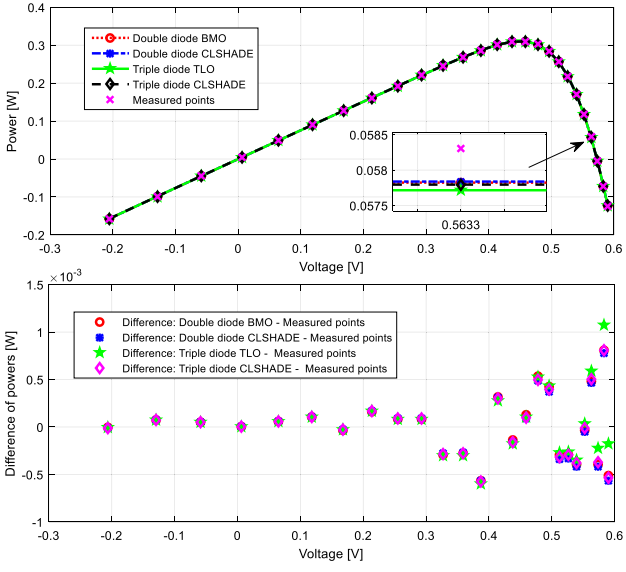
$$mean_{WL} = \frac{\sum_{k=1}^{|S|} \left(\frac{|f(u_{k,g}) - f(x_{k,g})|}{\sum_{l=1}^{|S_{CR}|} \Delta f_l} S_k^2 \right)}{\sum_{k=1}^{|S|} \left(\frac{|f(u_{k,g}) - f(x_{k,g})|}{\sum_{l=1}^{|S_{CR}|} \Delta f_l} \right)} \quad (38)$$

The overall pseudo-code of the LSHADE algorithm is presented in Table 6. The reader can refer to (Tanabe and Fukunaga, 2013; Tanabe and Fukunaga, 2014) for more detail about the SHADE and LSHADE algorithms. For further reading, the authors in (Mohamed et al., 2019; Stanovov et al., 2019) introduced different mutation strategies and exploitation improvements to enhance LSHADE algorithms' performance in solving global optimization problems. However, the LSHADE algorithm, as well as all the meta-heuristic algorithms, are random based optimization techniques. The randomness can be replaced by the chaos maps to benefit from their better statistical and dynamical properties. This can be simply realized by tuning some of the $rand$ parameters with chaos theory to avoid trapping in local minima (Zhang et al., 2018).

In this work, the previously described LSHADE algorithm is



(a)



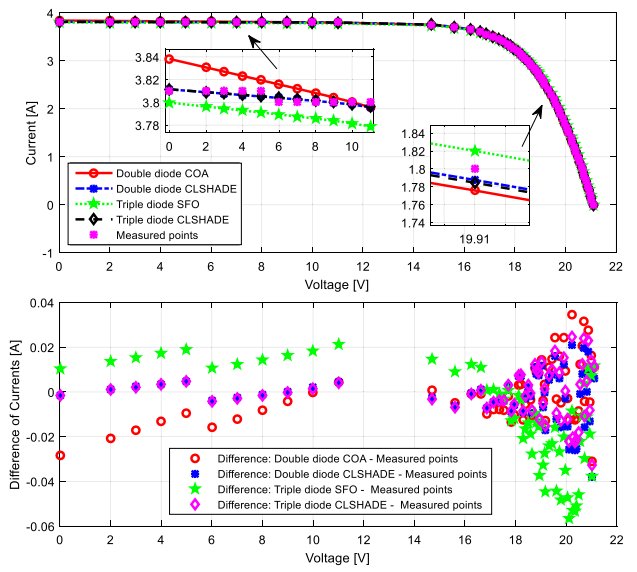
(b)

Fig. 7. Characteristic curves of the RTC France solar cell: (a) I - V , and (b) P - V

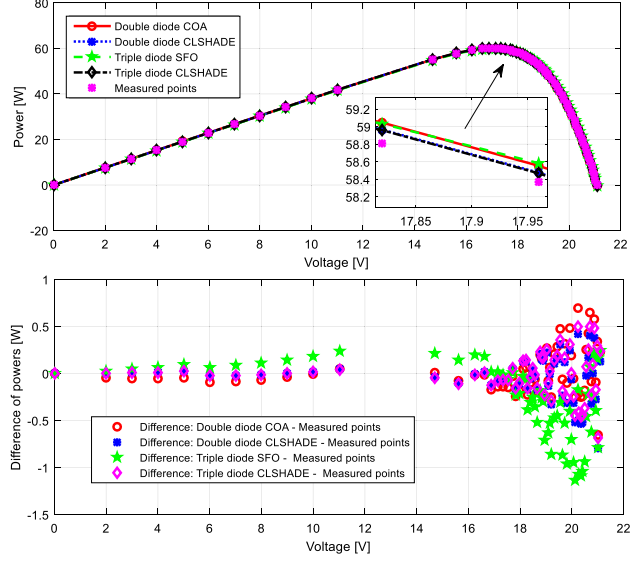
employed by replacing the random initial population with chaotic maps (Čalasan et al., 2019). In which, in the initialization process, the chaotic array represented in (39) is employed.

$$y_{k+1} = 4y_k(1 - y_k) \quad (39)$$

The logistic map generates chaotic sequences in the range of (0,1). In that way, the LSHADE algorithm's chaotic character is achieved, and it is called Chaotic LSHADE (CLSHADE). This kind of chaotic map has a much higher possibility of generating values near 0 and 1. Furthermore, the probability that the random map provides different random values between 0 and 1 is almost identical. The logistic map also makes local search faster than random maps while maintaining the algorithm's globality potential. The flow chart of the CLSHADE algorithm is



(a)



(b)

Fig. 8. Characteristic curves of the Solarex MSX-60 PV module: (a) I - V , and (b) P - V

illustrated in Fig. 6.

5. Numerical results of the optimization problem and experimental validation

This section is divided into three subsections. In the first subsection, the formulation of the optimization problem is presented. In the second subsection, the CLSHADE algorithm is employed to get the optimal parameters of the RTC France solar cell and Solarex MSX-60 PV module for both DDM and TDM. In the third subsection, the proposed method's applicability has been tested on experimentally-measured results of solar cells from the CETS.

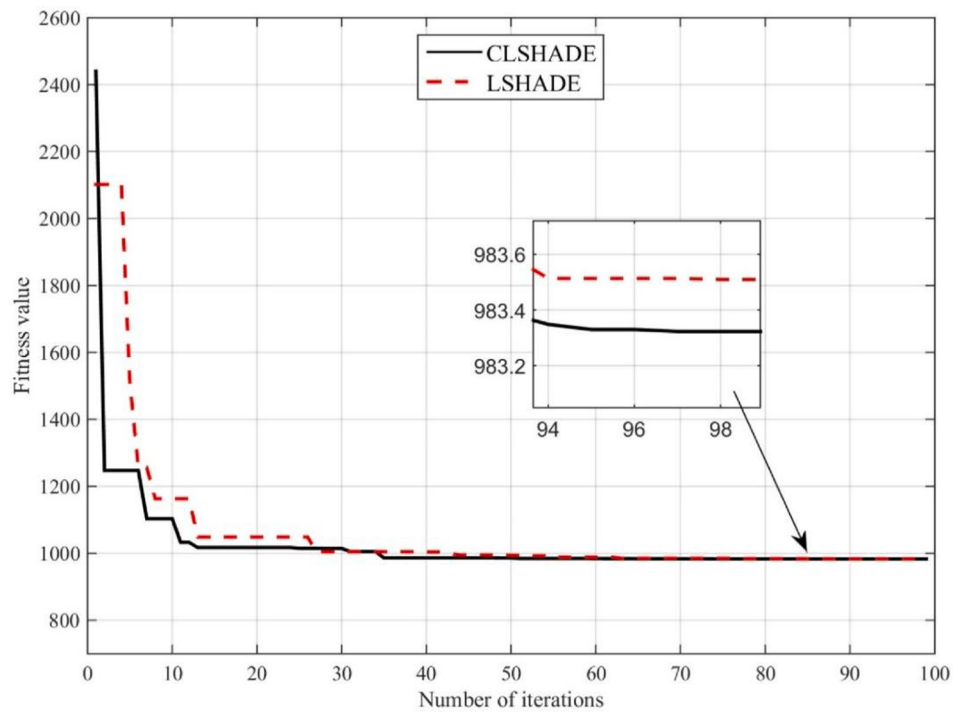


Fig. 9. Convergence curve of the CLSHADE and LSHADE algorithms: RTC France solar cell.

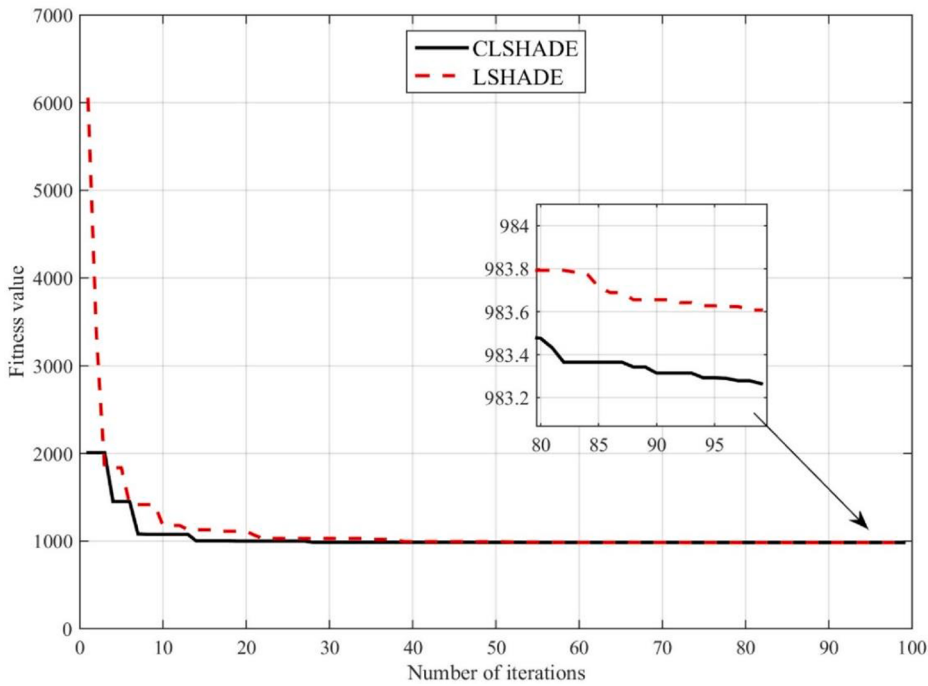


Fig. 10. Convergence curve of the CLSHADE and LSHADE algorithms: Solarex MSX-60 PV module.

5.1. Formulation of the optimization problem

To evaluate the performance of the CLSHADE for DDM and TDM parameters estimation, we applied the methodology proposed, and the CLSHADE improved to experimental *I*-*V* characteristics extracted from the manufacturer's datasheets of the RTC France solar cell. Then, we applied the proposed method to practical *I*-*V* characteristics extracted from the Solarex MSX-60 PV module. For both solar cells and modules, the range of unknown parameters, lower bound (LB) and upper bound

(UB), is given in Table 7 (Ćalasan et al., 2019; Premkumar et al., 2020).

The optimization problem is formulated as follows:

$$\text{minimize } f(x) = \begin{cases} RMSE_{DDM}(I_{PV}, I_{01}, n_1, I_{02}, n_2, R_P, R_S) \\ RMSE_{TDM}(I_{PV}, I_{01}, n_1, I_{02}, n_2, I_{03}, n_3, R_P, R_S) \end{cases} \quad (40)$$

s.t.:

$$LB \leq x \leq UB \quad (41)$$

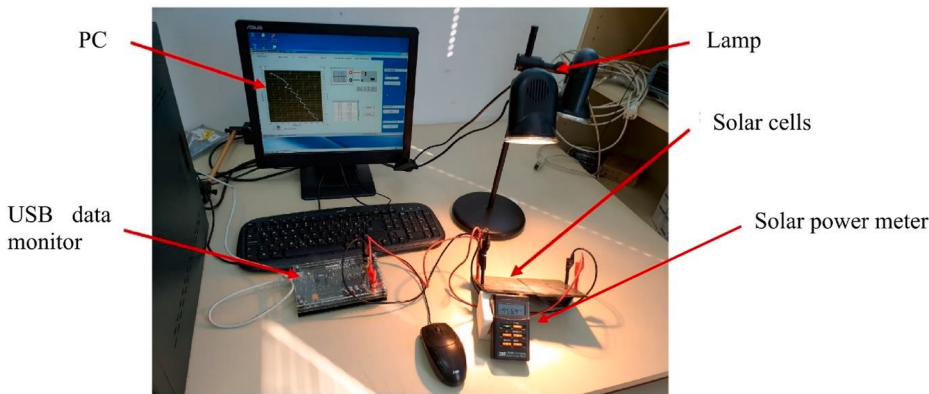


Fig. 11. Experimental setup of CETs.

Table 9
Boundaries for DDM and TDM parameters of the solar modules of CETs.

Variables	Range of the unknown parameters	
	LB	UB
I_{PV} (A)	0.20	0.40
I_01 (μ A)	0.10	2.00
I_02 (μ A)	1.00×10^{-6}	1.00×10^{-3}
I_03 (μ A)	1.00×10^{-6}	1.00×10^{-3}
R_S (Ω)	0.05	0.20
R_P (Ω)	200	600
n_1	0.20	0.80
n_2	1.00	2.00
n_3	1.00	2.00

Table 10
Optimal DDM parameters for the solar modules of CETs using the CLSHADE and LSHADE algorithms.

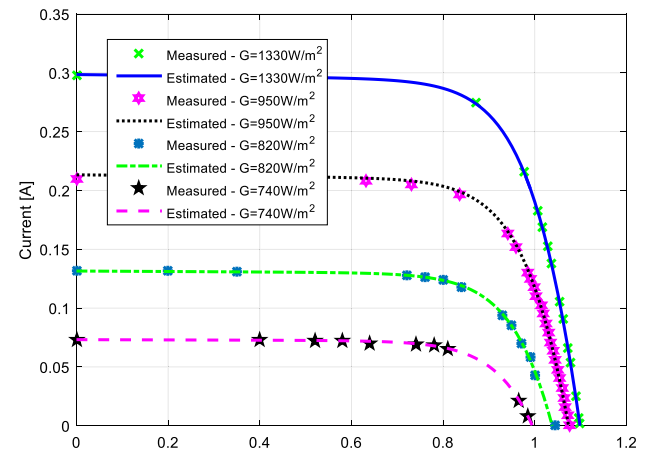
Variables	CLSHADE	LSHADe
I_{PV} (A)	0.29820	0.29800
I_01 (μ A)	0.12170	0.14199
I_02 (μ A)	1.000×10^{-5}	2.216×10^{-4}
R_S (Ω)	0.1079	0.1053
R_P (Ω)	348.8400	474.7970
n_1	0.3471	0.3508
n_2	1.9500	1.9723
Conventional RMSE	0.0012	0.0012
Proposed RMSE	1.127×10^{-5}	1.131×10^{-5}

Table 11
Optimal TDM parameters for the solar modules of CETs using the CLSHADE and LSHADE algorithms.

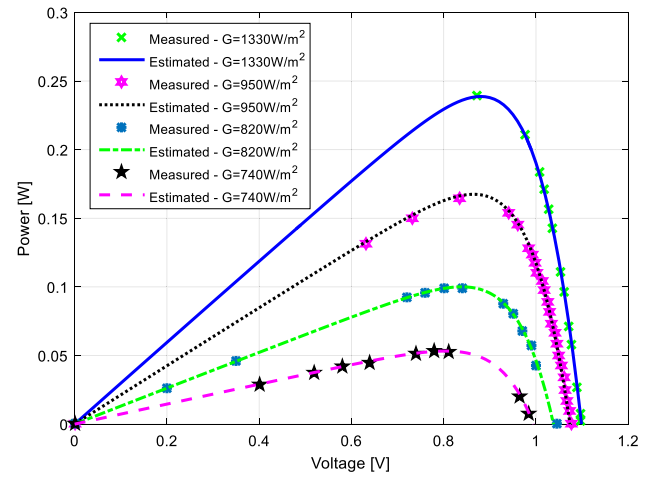
Variables	CLSHADE	LSHADe
I_{PV} (A)	0.29800	0.29809
I_01 (μ A)	0.11830	0.11300
I_02 (μ A)	2.470×10^{-4}	1.000×10^{-4}
I_03 (μ A)	2.467×10^{-4}	6.310×10^{-4}
R_S (Ω)	0.1087	0.1092
R_P (Ω)	378.4630	333.5600
n_1	0.3465	0.3546
n_2	2.0000	1.9910
n_3	1.9973	1.9288
Conventional RMSE	0.0012	0.0012
Proposed RMSE	1.123×10^{-5}	1.124×10^{-5}

5.2. Numerical results of the optimization problem

The values of parameters obtained using CLSHADE are summarized in Table 8 for the RTC France solar cell and Solarex MSX–60 PV module. The presented results, particularly the RMSE values, show that the



(a)



(b)

Fig. 12. Estimated and measured characteristic curves of the solar modules of CETs: (a) I-V, and (b) P-V

CLSHADE provides closer solar characteristics than the characteristics provided by the methods given in Tables 1–4, which indicates that the CLSHADE outperforms the other techniques presented in the literature in terms of accuracy of the solution. The measured and simulated I-V and P-V characteristics obtained using the optimal parameters found by the CLSHADE algorithm for DDM and TDM equivalent circuits are shown in

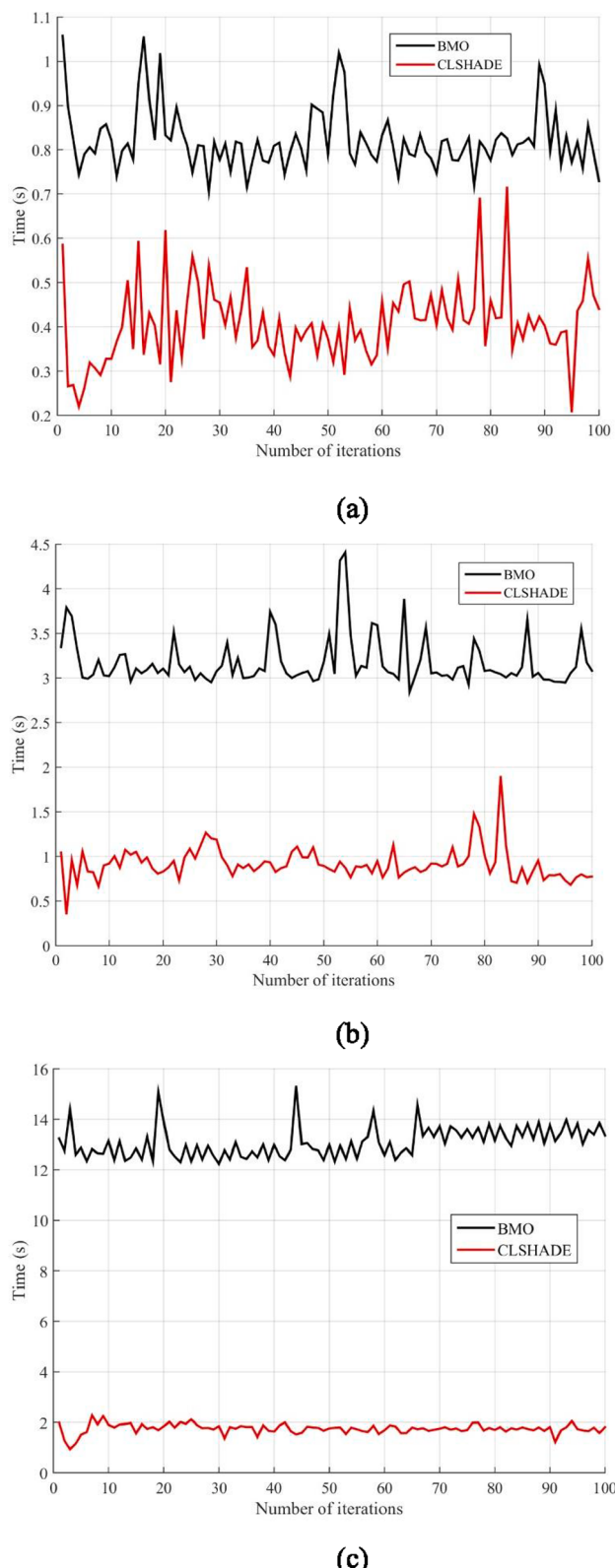


Fig. 13. Comparison of BMO and CLSHADE algorithms over 20 independent runs when population size/maximum number of iterations is: (a) 100/100, (b) 200/200, and (c) 400/400.

Fig. 7 for the RTC France cell and **Fig. 8** for the Solarex module. In the same figures, the measured and simulated *I*-*V* and *P*-*V* characteristics obtained using the DDM parameters estimated using the most accurate method presented in **Table 1** for parameter estimation of the double diode RTC France solar cell, i.e., BMO method (Askarzadeh and Reza-zadeh, 2013b) (method number 82) are given. Also, the measured and simulated *I*-*V* and *P*-*V* characteristics obtained using the TDM parameters estimated using the most accurate method presented in **Table 3** for parameter estimation of the triple diode RTC France solar cell, i.e., TLO method (Premkumar et al., 2020) (method number 6), are given.

From **Figs. 7 and 8**, all the presented methods enable perfect matching between measured and estimated curves. Besides, looking at the visualization of the difference of current between the considered methods, it can be seen that the CLSHADE outperforms other methods in terms of approaching the measured characteristics, in which the actual reasons for obtaining better results in this study compared to previous studies is the proposed RMSE expression that facilitates accurate results and the excellent performance of the CLSHADE algorithm. Moreover, to validate the performance of the CLSHADE algorithm, **Figs. 9 and 10** show the convergence curve's mean value over 100 iterations for the conventional LSHADE and CLSHADE algorithms of the RTC France solar cell and Solarex MSX-60 PV module, respectively. It can be seen that the CLSHADE is faster in convergence than the conventional LSHADE due to its chaotic nature.

5.3. Experimental validation

The proposed solution methodology is applied to *I*-*V* characteristics measured in the laboratory for solar modules of CETS to check the accuracy and efficiency of the CLSHADE algorithm and the iterative Lambert W procedure proposed for solar cell parameters estimation, and the 7 and 9 unknown parameters are estimated using the CLSHADE algorithm based on RMSE minimization.

In this regard, we conducted many experiments on one solar cell and two series-connected solar cells with different irradiance values. Irradiance was measured using TES1333R solar meter recording data (range 2000 W/m², resolution 0.1 W/m²). The irradiance has been altered using a particular dual spotlight bulb that simulates sunlight and provides the optimal light spectrum. The experimental setup is given in **Fig. 11**.

We measured the *I*-*V* characteristics for irradiance of 1330 W/m² and a temperature of 42 °C for the measured *I*-*V* pairs. Then, we determined the double and triple diode solar cell parameters for the solar modules of CETS. The range of the unknown parameters is given in **Table 9**.

The parameter values obtained using the CLSHADE and LSHADE for the solar modules of CETS for the DDM and TDM equivalent circuits are summarized in **Tables 10 and 11**, respectively.

It is evident from **Tables 10, 11** that the two optimization techniques' results are close. However, the CLSHADE algorithm provided better accuracy in terms of the proposed RMSE for both the DDM and TDM parameters. Also, differences between the conventional and proposed RMSE values are significant, which indicates the importance of the proposed iterative Lambert W procedure in obtaining better fitness function values.

The simulated and measured *I*-*V* and *P*-*V* characteristics at different irradiance values at $T = 42$ °C, using the TDM parameters obtained using the CLSHADE algorithm, presented in **Table 11**, are illustrated in **Fig. 12**. The agreement between the measured and estimated characteristics is evident. Moreover, to validate the CLSHADE algorithm's performance, we compared the CLSHADE and BMO algorithms' computation time for 20 independent runs with different population size values and the number of iterations, i.e., when population size/maximal number of

iterations is 100/100, 200/200, and 400/400. The results obtained are presented in Fig. 13. It can be seen that for a higher number of population size and the maximum number of iterations, the BMO requires much more computation time.

The CLSHADE is a more effective method as it required a lower value of time and better convergence than the BMO algorithm, which provided the best RMSE results for the DDM in the literature.

Finally, this work aimed to develop a good base for applying optimization methods to solve the parameter estimation problem of 7-parameter double diode and 9-parameter triple diode PV equivalent circuits.

6. Conclusions

No exact analytical solution has been reached for the current expressions of the DDM and TDM because of the high nonlinearity of these models' current expressions. Consequently, in the literature, an approximated expression for the calculated solar cell current is usually used in DDM and TDM parameters estimation. However, in the mathematical sense, the RMSE is not correctly calculated.

Accordingly, in this work, a novel iterative procedure based on the Lambert W function is proposed to calculate the solar cell current in both DDM and TDM, and its efficiency and accuracy are discussed. Further,

the RMSE values computed using the parameters found by many optimization algorithms presented in the literature are presented and discussed for the RTC France PV cell and Solarex MSX-60 PV module. The results obtained show that RMSE values were not accurately calculated in most of these methods. The CLSHADE optimization algorithm is proposed to solve the 7-parameter and 9-parameter estimation problem of the PV equivalent circuits of the RTC France cell and Solarex module based on the minimization of the RMSE expression proposed in this work. The results obtained show that the CLSHADE algorithm's accuracy, or any optimization technique that relies on RMSE calculation, can be improved using the proposed solar cell current expressions and the RMSE calculated based on them.

Funding

This research did not receive any specific grant from funding agencies in the public, commercial, or not-for-profit sectors.

Declaration of Competing Interest

The authors declare that they have no known competing financial interests or personal relationships that could have appeared to influence the work reported in this paper.

Appendix A

A.1. Matlab code for solving the iterative Lambert W equation

The Matlab code used for solving (11) using the iterative Lambert W equation is given below.

```
clear all
% define parameters of solar cell - Vt, Ioa, Io2, n1, n2 (ideality
% factors), Rp, Rs,Ipv
% Uiz - measured points of solar cell voltage
% Iiz - measured points of solar cell currents
RMSE = 0;
for t = 1:length(Uiz)
ALFA=((Rs/Vt/n1)/(1 + Rs/Rp))*(Io1*exp(Uiz(t)/Vt/n1))*exp((Rs/Vt/n1)*(Ipv + Io1 + Io2-Uiz(t)/Rp)/(1 + Rs/Rp));
BETA=((Rs/Vt/n1)/(1 + Rs/Rp))*(Io2*exp(Uiz(t)/Vt/n2))*exp((Rs/Vt/n2)*(Ipv + Io1 + Io2-Uiz(t)/Rp)/(1 + Rs/Rp));
DELTA = 1-n1/n2;
initial = 0; % DEFINE INITIAL VALUE
for counter = 1:1000% DEFINE UPPER LIMIT FOR COUNTER
current_iteration = counter;
TETA = ALFA + BETA*exp(DELTA*initial);
y = lambertw(TETA);
if abs(TETA-(ALFA + BETA*exp(DELTA*y))) < 1e-15
break
end
initial = y;
end
CURRENT=((Ipv + Io1 + Io2-Uiz(t)/Rp)-(y/((Rs/Vt/n1)/(1 + Rs/Rp)))/(1 + Rs/Rp);
CHECK=(Ipv-Io1*(exp((Uiz(t) + CURRENT*Rs)/Vt/n1)-1)-Io2*(exp((Uiz(t) + CURRENT*Rs)/Vt/n2)-1)-(Uiz(t) +
CURRENT*Rs)/Rp-struja;
RMSE = RMSE+(CURRENT-Iiz(t))^2;
end
```

A.2. Numerical example of solving the iterative Lambert W equation

Table A2.1 presents numerical results of solving (11) using two sets of α , β , and δ values and different initial values (0, 10, and 100). Besides, Fig. A2.1 shows a visualization of the solutions obtained using the results presented in Table A2.1.

Also, Table A2.2 presents numerical results of solving (18) using two sets of α , β , δ , γ , and σ values and different initial values (0, 10, and 100). Besides, Fig. A2.2 shows a visualization of the solutions obtained using the results presented in Table A2.2.

Table A2.1

Numerical results of solving (11) with different initial values.

Parameters	Iteration number	Initial value		
		0	10	100
$\alpha = 2.0$	1	0.958586356728703	1.108593324535639	7.316853954693936
	2	0.968361495093371	0.969963965500666	1.056583495937813
	3	0.968465306043657	0.968482332244302	0.96940607816970
	4	0.968466408962525	0.968466589854937	0.968476404448120
	5	0.968466420680319	0.968466422602183	0.968466526875892
	6	0.968466420804813	0.968466420825232	0.968466421933072
	7	—	—	0.968466420818123
$\alpha = 10.00$	1	1.745591577117192	1.914189314744880	68.860166840220216
	2	1.745784868064482	1.745821951307602	44.387422051028238
	3	1.745784907780387	1.745784915400662	25.368667511811388
	4	1.745784907788548	1.745784907790114	10.990190935472709
	5	—	—	2.077281196054134
	6	—	—	1.745862908901437
	7	—	—	1.745784923817344
	8	—	—	1.745784907791843

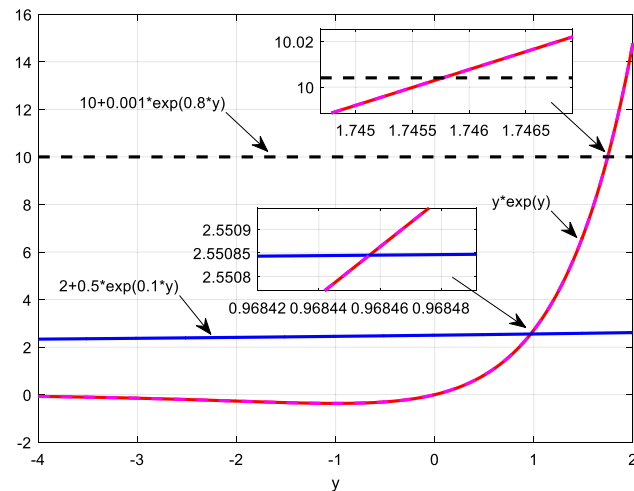
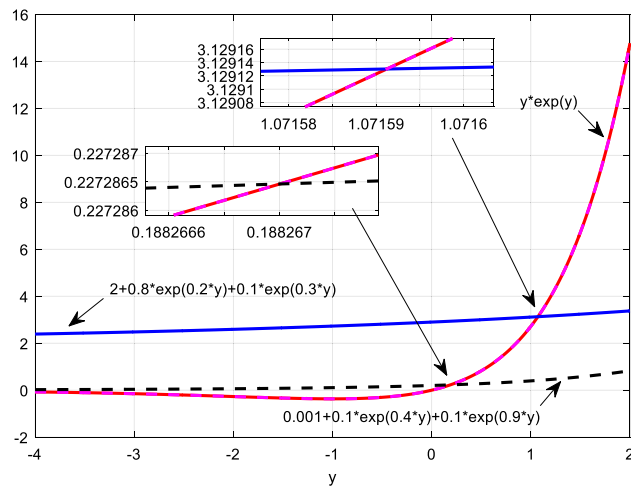


Fig. A2.1. Visualization of the solutions obtained using the results presented in Table A2.1.

Table A2.2

Numerical results of solving (18) with different initial values.

Parameters	Iteration number	Initial value		
		0	10	50
$\alpha = 2.0$	1	1.032615669166067	1.740411205492698	10.407404180868580
$\beta = 0.8$	2	1.070061976435101	1.099533289529359	1.787699586513120
$\gamma = 0.1$	3	1.071540528284446	1.072710380272906	1.101619953906888
$\delta = 0.2$	4	1.071599088725634	1.071645432336736	1.072793416778118
$\sigma = 0.3$	5	1.071601408389390	1.071603244142106	1.071648722149224
	6	1.071601500275070	1.071601572992264	1.071603374457933
	7	1.071601503914813	1.071601506795260	1.071601578154290
	8	1.071601504058989	1.071601504173088	1.071601506999737
	9	–	1.071601504069219	1.071601504181188
	10	–	–	1.071601504069540
$\alpha = 0.001$	1	0.169638022218497	5.079014278279280	39.033007278363492
$\beta = 0.100$	2	0.186345044460752	1.772295147387187	29.444610570233721
$\gamma = 0.100$	3	0.188079057277713	0.446163555898217	21.146108911291549
$\delta = 0.400$	4	0.188259967379910	0.217240003388225	14.083905809876400
$\sigma = 0.900$	5	0.188278851978195	0.191328961530911	8.262122666374754
	6	0.188280823389038	0.188599507598419	3.811299129613861
	7	0.188281029190798	0.188314300641855	1.137599308053954
	8	0.188281050675103	0.188284524021118	0.317976926842677
	9	0.188281052917918	0.188281415512003	0.202325634165605
	10	0.188281053152053	0.188281091004416	0.189753029229959
	11	–	0.188281057128024	0.188434781252588
	12	–	0.188281053591559	0.188297102041383
	13	–	0.188281053222376	0.188282728579105
	14	–	–	0.188281228079781
	15	–	–	0.188281071437762
	16	–	–	0.188281055085399
	17	–	–	0.188281053378323
	18	–	–	0.188281053200116

**Fig. A2.2.** Visualization of the solutions obtained using the results presented in Table A2.2.

A.3. The double diode and triple diode solar cell parameters

The double diode and triple diode solar cell parameters' values using the different methods addressed in Tables 1–4 are given in Table A3.1 and Table A3.3 for the RTC solar cell, and Table A3.2 and Table A3.4 for the Solarex MSX–60 PV module, respectively.

Table A3.1

Double diode model parameters of the RTC France solar cell.

No.	Ref.	Algorithm	R_S (Ω)	R_P (Ω)	I_{PV} (A)	I_{01} (μA)	I_{02} (μA)	n_1	n_2
1	(Yuan et al., 2014)	MPCOA	0.03635	54.2531	0.76078	0.31259	0.045280	1.47844	1.78459
2	(Askarzadeh and Rezazadeh, 2013a)	ABSO	0.03657	54.6219	0.76078	0.26713	0.381910	1.46512	1.98152
3	(Askarzadeh and Rezazadeh, 2012)	HS	0.03545	46.8270	0.76176	0.12545	0.254700	1.49439	1.49989
4		GGHS	0.03562	62.7899	0.76056	0.37014	0.135040	1.49638	1.92998
5		IGHS	0.03690	56.8368	0.76079	0.97310	0.167910	1.92126	1.42814
6	(El-Naggar et al., 2012)	SA	0.03450	43.1034	0.76230	0.47670	0.010000	1.51720	2.00000
7	(Alam et al., 2015)	FPA	0.03633	52.3475	0.76080	0.30009	0.166160	1.47477	2.00000
8	(Chen et al., 2018b)	EDDM-LW	0.03723	55.9729	0.76083	0.08528	0.929490	1.37994	1.79120
9	(Jordehi, 2016)	TVAPSO	0.03797	56.5496	0.76081	0.04047	0.927470	1.32716	1.73532
10		ICA	0.03602	58.5044	0.76070	0.36544	0.004710	1.49198	1.67008
11		TLBO	0.03611	51.1160	0.76093	0.32994	0.000010	1.48132	1.77314
12		GWO	0.03642	53.1032	0.76108	0.00349	0.337890	1.68195	1.48381
13		WCA	0.03731	54.6698	0.76082	0.15845	0.999530	1.41960	1.94320
14		CPSO	0.03735	55.44152	0.76081	0.95757	0.133450	1.88107	1.40749
15		PS	0.05861	18.21063	0.76335	0.00029	0.000001	1.00012	1.00091
16	(Ram et al., 2017)	BPFPA	0.03640	59.62400	0.76000	0.32110	0.045280	1.47930	2.00000
17	(Abd Elaziz and Oliva, 2018)	OBWAO	0.03671	55.39900	0.76076	0.22990	0.619560	1.49154	2.00000
18	(Merchaoui et al., 2018)	MPSO	0.03799	58.24134	0.76081	0.00897	2.136189	1.37364	2.00000
19	(Chen et al., 2019a)	ISCA	0.03674	55.48543	0.76078	0.74935	0.225974	2.00000	1.45102
20	(Yousri et al., 2019)	HCLPSO	0.03764	55.79600	0.76081	0.08797	0.973760	1.37950	1.81700
21	(AlHajri et al., 2012)	PS	0.03200	81.30080	0.76020	0.98890	0.000100	1.60000	1.19200
22	(Chellaswamy and Ramesh, 2016)	DET	0.03685	54.53210	0.76098	0.33267	0.064700	1.48735	1.79560
23	(Xu and Wang, 2017)	GOFPANM	0.03674	55.48545	0.76078	0.74935	0.225974	2.00000	1.45102
24	(Rezaee, 2018)	ELPSO	0.03755	55.92047	0.76081	1.00000	0.099168	1.83576	1.38609
25		BSA	0.03539	54.45518	0.76162	0.41639	0.000001	1.50537	2.00000
26		ABC	0.03666	58.29956	0.76072	0.28670	0.247485	1.46915	1.96837
27		GA	0.02914	51.11600	0.76886	0.66062	0.455149	1.60874	1.62890
28	(Premkumar et al., 2020)	R-II	0.03675	55.71854	0.76078	0.74911	0.226410	2.00000	1.45471
29		R-III	0.03674	55.71851	0.76078	0.74814	0.219110	2.00000	1.45145
30		PSO	0.03538	53.41254	0.76111	0.19781	0.425890	1.68418	1.48345
31	(Kang et al., 2018)	ImCSA	0.03674	55.48269	0.76078	0.22597	0.747309	1.45154	2.00000
32	(Jamadi et al., 2016)	MABC	0.03671	54.75501	0.76078	0.63069	0.241030	2.00001	1.45686
33	(Wu et al., 2018)	ABC-TRR	0.03674	55.48544	0.76078	0.22597	0.749349	1.45102	2.00000
34		ABC-KP	0.03766	48.56321	0.76148	0.06334	1.000000	1.35721	1.78647
35	(Guo et al., 2016)	CSO	0.03674	55.38130	0.76078	0.22732	0.727850	1.45151	1.99769
36	(Gong and Cai, 2013)	Rcr-IJADE	0.03674	55.48544	0.76078	0.22597	0.749347	1.45102	2.00000
37	(Chen et al., 2016a)	GOTLBO	0.03678	56.07530	0.76075	0.80020	0.220462	1.99997	1.44897
38	(Chen et al., 2016b)	EHA-NMS	0.03674	55.48831	0.76078	0.22587	0.750729	1.45087	2.00000
39	(Hamid et al., 2016)	NM-MPSO	0.03675	55.52960	0.76078	0.22476	0.755240	1.45054	1.99998
40	(Yu et al., 2017a)	SATLBO	0.03663	55.11700	0.76078	0.25093	0.545418	1.45982	1.99941
41	(Oliva et al., 2017)	CWOA	0.03666	55.20160	0.76077	0.24150	0.600000	1.45651	1.98990
42	(Yu et al., 2017b)	IJAYA	0.03760	77.85190	0.76010	0.00504	0.750940	1.21860	1.62470
43		LETI-LBO	0.03650	54.30210	0.76080	0.17390	0.226640	1.65850	1.45780
44		LBSA	0.03650	56.05240	0.76070	0.24877	0.274360	1.88170	1.46820
45	(Yu et al., 2019)	PGJAYA	0.03680	55.81350	0.76080	0.21031	0.885340	1.44500	2.00000
46		GOTLBO	0.03650	53.40580	0.76080	0.13894	0.262090	1.72540	1.46580
47		JAYA	0.03640	52.65750	0.76070	0.00608	0.315070	1.84360	1.47880
48		STLBO	0.03670	55.33820	0.76080	0.23364	0.684940	1.45380	2.00000
49		TLABC	0.03610	55.06760	0.76080	0.33673	0.071730	1.48610	1.93160
50		CLPSO	0.03670	57.94220	0.76070	0.25843	0.386150	1.46250	1.94350
51		BLPSO	0.03660	61.13450	0.76080	0.27189	0.435050	1.46740	1.96620
52		DE/BBO	0.03580	58.40180	0.76060	0.00122	0.372200	1.87910	1.49560
53		CMM-DE/BBO	0.03600	57.98820	0.76070	0.35366	0.025623	1.49070	1.88350
54	(Chen et al., 2018a)	TLBO	0.03661	53.12099	0.76099	0.29465	0.137270	1.47295	1.99375
55		NIWTLBO	0.03651	53.70554	0.76080	0.28430	0.270810	1.47026	1.99960
56		LETI-LBO	0.03642	54.06878	0.76081	0.11366	0.303170	1.92836	1.47597
57		GOTLBO	0.03655	53.61867	0.76081	0.27173	0.259520	1.46681	1.91606
58		ABC	0.03654	55.36509	0.76071	0.14623	0.246050	1.68023	1.46226
59		GABC	0.03638	52.98993	0.76089	0.32391	0.000070	1.48146	1.99282
60		MABC	0.03651	55.22908	0.76071	0.21750	0.165550	1.45606	1.63102
61		GBABC	0.03690	55.93810	0.76073	0.57372	0.216890	1.92862	1.44779
62		TLABC	0.03667	54.666797	0.76081	0.42394	0.240110	1.90750	1.45671
63	(Niu et al., 2014b)	TLBO	0.03646	55.84590	0.76067	0.20289	0.299480	1.99809	1.47494
64		STLBO	0.03674	55.49200	0.76078	0.22566	0.752170	1.45085	2.00000
65	(Niu et al., 2014a)	BBO-M	0.03664	55.04940	0.76083	0.59115	0.245230	2.00000	1.45798
66		BBO	0.03673	58.45850	0.75940	0.95830	0.148850	1.85714	1.42309
67		DE	0.03661	56.02130	0.76079	0.36605	0.263200	1.91164	1.46500
68	(Oliva et al., 2014)	ABC	0.03640	53.78040	0.76080	0.04070	0.287400	1.46512	1.48850
69	(Chen et al., 2019b)	CLPSO	0.03619	52.40069	0.76112	0.00237	0.338750	1.68481	1.48612
70		BLPSO	0.03553	64.79937	0.76056	0.17895	0.315600	1.69574	1.48789
71		IJAYA	0.03671	54.65515	0.76079	0.49461	0.220690	1.88559	1.45021
72		SFS	0.03669	55.30604	0.76078	0.65647	0.237210	1.99990	1.45509
73		pSFS	0.03679	55.72835	0.76078	0.84161	0.215450	2.00000	1.44705
74	(Beigi and Maroosi, 2018)	GA	0.03640	53.71850	0.76080	0.00010	0.000100	1.33550	1.48100

(continued on next page)

Table A3.1 (continued)

No.	Ref.	Algorithm	R_S (Ω)	R_P (Ω)	I_{PV} (A)	I_{01} (μA)	I_{02} (μA)	n_1	n_2
75		PSO	0.03250	43.10340	0.76230	0.47670	0.010000	1.51720	2.00000
76		BFA	0.03510	60.00000	0.76090	0.00940	0.045300	1.38090	1.52550
77		FA	0.03671	49.18670	0.76101	0.00000	0.292634	2.00000	1.47134
78		HFAPS	0.03674	55.48550	0.76078	0.22597	0.749358	1.45101	2.00000
79		ABC	0.03686	55.93352	0.76081	0.19268	0.999587	1.43800	1.98372
80	(Lin et al., 2017)	SSO	0.03626	55.85327	0.76065	0.28720	0.065979	1.51035	1.43384
81		MSSO	0.03669	55.71466	0.76075	0.23493	0.671593	1.45426	1.99531
82	(Askarzadeh and Rezazadeh, 2013b)	BMO	0.03682	55.80810	0.76078	0.21110	0.876880	1.44533	1.99997
83	(Mughal et al., 2017)	HPSOSA	0.03741	55.53928	0.76081	0.11199	0.855939	1.39593	1.82014
84		CPSO	0.03560	45.54753	0.76232	0.29711	0.710454	1.47604	1.99810
85	(Wang et al., 2015)	IABC	0.03641	55.23070	0.76090	0.26900	0.281890	1.46700	1.87220
86	(Čalasan et al., 2019)	COA	0.03674	55.48542	0.76078	0.22597	0.749346	1.45102	2.00000
87	(Chenouard and El-Sehiemy, 2020)	IBEXOPT-MAE	0.03575	72.55642	0.75964	0.21796	0.176366	1.50488	1.49902
88		IBEXOPT-SSE	0.03692	56.44978	0.76073	0.87556	0.189347	1.95378	1.43750
89	(Luu and Nguyen, 2020)	MJAYA	0.03674	55.48540	0.76080	0.22597	0.749350	1.45100	2.00000
90	(Xiong et al., 2020)	ODE	0.03670	55.31854	0.76078	6.80886	0.234062	1.99994	1.45396
91		RTLBO	0.03670	55.31038	0.76078	0.23433	0.678565	1.45405	2.00000
92		WLCSODGM	0.03674	55.48504	0.76078	0.74920	0.225992	2.00000	1.45102

Table A3.2

Double diode model parameters of the Solarex MSX-60 module.

No.	Ref.	Algorithm	R_S (Ω)	R_P (Ω)	I_{PV} (A)	I_{01} (μA)	I_{02} (μA)	n_1	n_2
1	(Kumar and Kumar, 2017)	Analytical	0.3084	280.6449	3.8752	3.61×10^{-10}	9.38×10^{-6}	1.0000	2.0000
2		Numerical	0.3397	280.2171	3.8046	3.99×10^{-10}	4.03×10^{-6}	0.9986	2.0014
3	(Ishaque et al., 2011)	Iteration method	0.3500	176.4000	3.8000	4.70×10^{-10}	4.70×10^{-10}	1.0000	1.2000
4	(Elbaset et al., 2014)	Newton method	0.3692	169.0471	3.8084	4.87×10^{-10}	6.15×10^{-10}	1.0003	1.9997
5	(Čalasan et al., 2019)	COA	0.2495	267.5700	3.8418	4.96×10^{-8}	9.55×10^{-9}	1.2569	1.9345

Table A3.3

Triple diode model parameters of the RTC France solar cell.

No.	Ref.	Algorithm	R_S (Ω)	R_P (Ω)	I_{PV} (A)	I_{01} (μA)	I_{02} (μA)	I_{03} (μA)	n_1	n_2	n_3
1	(Premkumar et al., 2020)	R-II	0.03660	54.9149	0.760792	0.2600	0.000006	0.5700	1.4608	1.1466	2.0208
2		R-III	0.03670	55.3571	0.760791	0.2100	0.220000	0.9900	1.7714	1.4513	2.4103
3		PSO	0.03660	55.3133	0.760782	0.2500	0.041000	1.0000	1.4601	1.7409	2.2514
4		CS	0.03630	53.7218	0.760776	0.1400	0.190000	0.0310	1.4872	1.4771	4.4663
5		ABC	0.03670	55.4411	0.760790	0.3200	0.230000	0.7400	1.8666	1.4521	2.3949
6		TLO	0.03650	55.3821	0.760763	0.2800	0.000670	1.0000	1.4684	1.5468	2.3225
7	(Abd Elaziz and Oliva, 2018)	ABC	0.03687	55.8344	0.760700	0.2000	0.500000	0.2100	1.4414	1.9000	2.0000
8		OBWOA	0.03668	55.4448	0.760770	0.2353	0.221300	0.4573	1.4543	2.0000	2.0000
9		STLBO	0.0367	55.2641	0.760800	0.2349	0.229700	0.4443	1.4541	2.0000	2.0000

Table A3.4

Triple diode model parameters of the Solarex MSX-60 module.

No.	Ref.	Algorithm	R_S (Ω)	R_P (Ω)	I_{PV} (A)	I_{01} (μA)	I_{02} (μA)	I_{03} (μA)	n_1	n_2	n_3
1	(Elazab et al., 2020)	GA	0.30676	193.6150	3.5885	0.12960	0.000320	0.000310	1.37590	1.23815	1.13000
2		SA	0.15505	230.8550	3.9825	0.32164	0.000186	0.000102	1.39350	1.47650	1.37950
3		WOA	0.16153	266.8166	3.7438	0.24415	0.000187	0.000465	1.39736	1.09209	1.41391
4	(Qais et al., 2019a)	SFO	0.20598	578.3468	3.8011	0.04980	0.000724	0.142000	1.28200	1.80430	1.43640
5		GA	0.18100	280.2200	3.8010	0.01640	0.000482	0.000129	1.21000	1.25000	1.30000
6		SA	0.21100	298.5900	3.7920	0.01980	0.000476	0.000262	1.29000	1.22000	1.28000
7		WOA	0.19500	277.3700	3.7560	0.02192	0.000368	0.000397	1.30000	1.23000	1.03000
8	(Qais et al., 2019b)	COOA	0.17140	258.9310	3.7060	0.02043	0.000154	0.000137	1.24370	1.00610	1.07570

References

- Abbassi, R., Abbassi, A., Jemli, M., Chebbi, S., 2018. Identification of unknown parameters of solar cell models: A comprehensive overview of available approaches. Renew. Sustain. Energy Rev. 90, 453–474.
- Abdel Aleem, S.H.E., Zobaa, A.F., Abdel Mageed, H.M., 2015. Assessment of energy credits for the enhancement of the Egyptian Green Pyramid Rating System. Energy Policy 87, 407–416.
- Abd Elaziz, M., Oliva, D., 2018. Parameter estimation of solar cells diode models by an improved opposition-based whale optimization algorithm. Energy Convers. Manag. 171, 1843–1859.
- Alam, D.F., Youssi, D.A., Eteiba, M.B., 2015. Flower Pollination Algorithm based solar PV parameter estimation. Energy Convers. Manag. 101, 410–422.
- AlHajri, M.F., El-Naggar, K.M., AlRashidi, M.R., Al-Othman, A.K., 2012. Optimal extraction of solar cell parameters using pattern search. Renew. Energy 44, 238–245.
- Askarzadeh, A., Rezazadeh, A., 2012. Parameter identification for solar cell models using harmony search-based algorithms. Sol. Energy 86, 3241–3249.
- Askarzadeh, A., Rezazadeh, A., 2013a. Artificial bee swarm optimization algorithm for parameters identification of solar cell models. Appl. Energy 102, 943–949.
- Askarzadeh, A., Rezazadeh, A., 2013b. Extraction of maximum power point in solar cells using bird mating optimizer-based parameters identification approach. Sol. Energy 90, 123–133.
- Baig, M.Q., Khan, H.A., Ahsan, S.M., 2020. Evaluation of solar module equivalent models under real operating conditions—A review. J. Renew. Sustain. Energy 12, 012701.
- Bana, S., Saini, R.P., 2016. A mathematical modeling framework to evaluate the performance of single diode and double diode based SPV systems. Energy Rep. 2, 171–187.

- Beigi, A.M., Maroosi, A., 2018. Parameter identification for solar cells and module using a Hybrid Firefly and Pattern Search Algorithms. *Sol. Energy* 171, 435–446.
- Calasan, M., Nedic, A., 2018. Experimental Testing and Analytical Solution by Means of Lambert W-Function of Inductor Air Gap Length. *Electr. Power Components Syst.* 46, 852–862.
- Čalasan, M.P., 2019. Analytical solution for no-load induction machine speed calculation during direct start-up. *Int. Trans. Electr. Energy Syst.* 29, e2777.
- Čalasan, M.P., Jovanović, R., Mujović, D., 2019. Estimation of Single-Diode and Two-Diode Solar Cell Parameters by Using a Chaotic Optimization Approach. *Energies* 12, 4209.
- Čalasan, M., Abdel Aleem, S.H.E., Zobaa, A.F., 2020a. On the root mean square error (RMSE) calculation for parameter estimation of photovoltaic models: A novel exact analytical solution based on Lambert W function. *Energy Convers. Manag.* 210, 112716.
- Čalasan, M., Micev, M., Ali, Z.M., Zobaa, A.F., Abdel Aleem, S.H.E., 2020b. Parameter Estimation of Induction Machine Single-Cage and Double-Cage Models Using a Hybrid Simulated Annealing-Evaporation Rate Water Cycle Algorithm. *Mathematics* 8, 1024.
- Chellaswamy, C., Ramesh, R., 2016. Parameter extraction of solar cell models based on adaptive differential evolution algorithm. *Renew. Energy* 97, 823–837.
- Chen, X., Yu, K., Du, W., Zhao, W., Liu, G., 2016a. Parameters identification of solar cell models using generalized oppositional teaching learning based optimization. *Energy* 99, 170–180.
- Chen, Z., Wu, L., Lin, P., Wu, Y., Cheng, S., 2016b. Parameters identification of photovoltaic models using hybrid adaptive Nelder-Mead simplex algorithm based on eagle strategy. *Appl. Energy*.
- Chen, X., Xu, B., Mei, C., Ding, Y., Li, K., 2018a. Teaching-learning-based artificial bee colony for solar photovoltaic parameter estimation. *Appl. Energy* 212, 1578–1588.
- Chen, Y., Sun, Y., Meng, Z., 2018b. An improved explicit double-diode model of solar cells: Fitness verification and parameter extraction. *Energy Convers. Manag.* 169, 345–358.
- Chen, H., Jiao, S., Heidari, A.A., Wang, M., Chen, X., Zhao, X., 2019a. An opposition-based sine cosine approach with local search for parameter estimation of photovoltaic models. *Energy Convers. Manag.* 195, 927–942.
- Chen, X., Yue, H., Yu, K., 2019b. Perturbed stochastic fractal search for solar PV parameter estimation. *Energy* 189, 116247.
- Chenouard, R., El-Sehiemy, R.A., 2020. An interval branch and bound global optimization algorithm for parameter estimation of three photovoltaic models. *Energy Convers. Manag.* 205, 112400.
- Elazab, O.S., Hasanien, H.M., Alsaidan, I., Abdelaziz, A.Y., Muyeen, S.M., 2020. Parameter Estimation of Three Diode Photovoltaic Model Using Grasshopper Optimization Algorithm. *Energies* 13, 497.
- Elbaset, A.A., Ali, H., Abd-El, S.M., 2014. Novel seven-parameter model for photovoltaic modules. *Sol. Energy Mater. Sol. Cells* 130, 442–455.
- El-Naggar, K.M., AlRashidi, M.R., AlHajri, M.F., Al-Othman, A.K., 2012. Simulated Annealing algorithm for photovoltaic parameters identification. *Sol. Energy* 86, 266–274.
- Gong, W., Cai, Z., 2013. Parameter extraction of solar cell models using repaired adaptive differential evolution. *Sol. Energy*.
- Guo, L., Meng, Z., Sun, Y., Wang, L., 2016. Parameter identification and sensitivity analysis of solar cell models with cat swarm optimization algorithm. *Energy Convers. Manag.* 108, 520–528.
- Hamid, N.F.A., Rahim, N.A., Selvaraj, J., 2016. Solar cell parameters identification using hybrid Nelder-Mead and modified particle swarm optimization. *J. Renew. Sustain. Energy* 8, 015502.
- Ishaque, K., Salam, Z., Taheri, H., 2011. Accurate MATLAB Simulink PV System Simulator Based on a Two-Diode Model. *J. Power Electron.* 11, 179–187.
- Jamadi, M., Merrikh-Bayat, F., Bigdeli, M., 2016. Very accurate parameter estimation of single- and double-diode solar cell models using a modified artificial bee colony algorithm. *Int. J. Energy Environ. Eng.* 7, 13–25.
- Jordehi, A.R., 2016. Time varying acceleration coefficients particle swarm optimisation (TVACPSO): A new optimisation algorithm for estimating parameters of PV cells and modules. *Energy Convers. Manag.* 129, 262–274.
- Kang, T., Yao, J., Jin, M., Yang, S., Duong, T., 2018. A Novel Improved Cuckoo Search Algorithm for Parameter Estimation of Photovoltaic (PV) Models. *Energies* 11, 1060.
- Kumar, M., Kumar, A., 2017. An efficient parameters extraction technique of photovoltaic models for performance assessment. *Sol. Energy* 158, 192–206.
- Lin, P., Cheng, S., Yeh, W., Chen, Z., Wu, L., 2017. Parameters extraction of solar cell models using a modified simplified swarm optimization algorithm. *Sol. Energy* 144, 594–603.
- Luu, T.V., Nguyen, N.S., 2020. Parameters extraction of solar cells using modified JAYA algorithm. *Optik (Stuttg.)* 203, 164034.
- Merchaoui, M., Sakly, A., Mimouni, M.F., 2018. Particle swarm optimisation with adaptive mutation strategy for photovoltaic solar cell/module parameter extraction. *Energy Convers. Manag.* 175, 151–163.
- Mohamed, A.W., Hadi, A.A., Jambi, K.M., 2019. Novel mutation strategy for enhancing SHADE and LSHADE algorithms for global numerical optimization. *Swarm Evol. Comput.* 50, 100455.
- Mostafa, M.H., Abdel Aleem, S.H.E., Ali, S.G., Ali, Z.M., Abdelaziz, A.Y., 2020. Techno-economic assessment of energy storage systems using annualized life cycle cost of storage (LCCOS) and levelized cost of energy (LCOE) metrics. *J. Energy Storage* 29, 101345.
- Mughal, M.A., Ma, Q., Xiao, C., 2017. Photovoltaic Cell Parameter Estimation Using Hybrid Particle Swarm Optimization and Simulated Annealing. *Energies* 10, 1213.
- Nishioka, K., Sakitani, N., Uraoka, Y., Fuyuki, T., 2007. Analysis of multicrystalline silicon solar cells by modified 3-diode equivalent circuit model taking leakage current through periphery into consideration. *Sol. Energy Mater. Sol. Cells* 91, 1222–1227.
- Niu, Q., Zhang, L., Li, K., 2014a. A biogeography-based optimization algorithm with mutation strategies for model parameter estimation of solar and fuel cells. *Energy Convers. Manag.* 86, 1173–1185.
- Niu, Q., Zhang, H., Li, K., 2014b. An improved TLBO with elite strategy for parameters identification of PEM fuel cell and solar cell models. *Int. J. Hydrogen Energy* 39, 3837–3854.
- Oliva, D., Cuevas, E., Pajares, G., 2014. Parameter identification of solar cells using artificial bee colony optimization. *Energy* 72, 93–102.
- Oliva, D., Abd El Aziz, M., Ella, H.A., 2017. Parameter estimation of photovoltaic cells using an improved chaotic whale optimization algorithm. *Appl. Energy* 200, 141–154.
- Peng, L., Sun, Y.Z., Meng, Z., 2013. An Improved Model of Photovoltaic Cell Using Lambert W Function. *Appl. Mech. Mater.* 368–370, 1196–1200.
- Premkumar, M., Babu, T.S., Umashankar, S., Sowmya, R., 2020. A new metaphor-less algorithms for the photovoltaic cell parameter estimation. *Optik (Stuttg.)* 208, 164559.
- Qais, M.H., Hasanien, H.M., Alghuwainem, S., 2019a. Identification of electrical parameters for three-diode photovoltaic model using analytical and sunflower optimization algorithm. *Appl. Energy* 250, 109–117.
- Qais, M.H., Hasanien, H.M., Alghuwainem, S., Nouh, A.S., 2019b. Coyote optimization algorithm for parameters extraction of three-diode photovoltaic models of photovoltaic modules. *Energy* 187, 116001.
- Ram, J.P., Babu, T.S., Dragicevic, T., Rajasekar, N., 2017. A new hybrid bee pollinator flower pollination algorithm for solar PV parameter estimation. *Energy Convers. Manag.* 135, 463–476.
- Rezaee, J.A., 2018. Enhanced leader particle swarm optimisation (ELPSO): An efficient algorithm for parameter estimation of photovoltaic (PV) cells and modules. *Sol. Energy* 159, 78–87.
- Stanovov, V., Akhmedova, S., Semenkin, E., 2019. Selective Pressure Strategy in differential evolution: Exploitation improvement in solving global optimization problems. *Swarm Evol. Comput.* 50, 100463.
- Tanabe, R., Fukunaga, A., 2013. Success-history based parameter adaptation for Differential Evolution. 2013 IEEE Congr. Evol. Comput. CEC 2013.
- Tanabe, R., Fukunaga, A.S., 2014. Improving the search performance of SHADE using linear population size reduction. 2014 IEEE Congr. Evol. Comput., IEEE. p. 1658–65.
- Wang, R., Zhan, Y., Zhou, H., 2015. Application of Artificial Bee Colony in Model Parameter Identification of Solar Cells. *Energies* 8, 7563–7581.
- Wu, H., Peng, L., 2018. A Maximum Power Point Detection Method for Photovoltaic Module Based on Lambert W Function. *Math. Prob. Eng.* 2018, 1–8.
- Wu, L., Chen, Z., Long, C., Cheng, S., Lin, P., Chen, Y., et al., 2018. Parameter extraction of photovoltaic models from measured I-V characteristics curves using a hybrid trust-region reflective algorithm. *Appl. Energy* 232, 36–53.
- Xiong, G., Zhang, J., Shi, D., Zhu, L., Yuan, X., Tan, Z., 2020. Winner-leading competitive swarm optimizer with dynamic Gaussian mutation for parameter extraction of solar photovoltaic models. *Energy Convers. Manag.* 206, 112450.
- Xu, S., Wang, Y., 2017. Parameter estimation of photovoltaic modules using a hybrid flower pollination algorithm. *Energy Convers. Manag.* 144, 53–68.
- Yousri, D., Allam, D., Eteiba, M.B., Suganthan, P.N., 2019. Static and dynamic photovoltaic models' parameters identification using Chaotic Heterogeneous Comprehensive Learning Particle Swarm Optimizer variants. *Energy Convers. Manag.* 182, 546–563.
- Yu, K., Chen, X., Wang, X., Wang, Z., 2017a. Parameters identification of photovoltaic models using self-adaptive teaching-learning-based optimization. *Energy Convers. Manag.* 145, 233–246.
- Yu, K., Liang, J.J., Qu, B.Y., Chen, X., Wang, H., 2017b. Parameters identification of photovoltaic models using an improved JAYA optimization algorithm. *Energy Convers. Manag.* 150, 742–753.
- Yu, K., Qu, B., Yue, C., Ge, S., Chen, X., Liang, J., 2019. A performance-guided JAYA algorithm for parameters identification of photovoltaic cell and module. *Appl. Energy* 237, 241–257.
- Yuan, X., Xiang, Y., He, Y., 2014. Parameter extraction of solar cell models using mutative-scale parallel chaos optimization algorithm. *Sol. Energy* 108, 238–251.
- Zhang, Q., Chen, H., Luo, J., Xu, Y., Wu, C., Li, C., 2018. Chaos enhanced bacterial foraging optimization for global optimization. *IEEE Access* 6, 64905–64919.
- Zobaa, A.F., Aleem, S.H.E.A., Abdelaziz, A.Y., 2018. Classical and Recent Aspects of Power System Optimization. Elsevier.